Contrasting physiological strategies explain heterogeneous responses to severe drought conditions within local populations of a widespread conifer

Journal Article

Author(s):
Depardieu, Claire; Lenz, Patrick; Marion, Joelle; Nadeau, Simon; Girardin, Martin P.; Marchand, William; Bégin, Christian; Treydte, Kerstin; Gessler, Arthur; Bousquet, Jean; Savard, Martine M.; Isabel, Nathalie

Publication date:
2024-05-01

Permanent link:
https://doi.org/10.3929/ethz-b-000666224

Originally published in:
Science of The Total Environment 923, https://doi.org/10.1016/j.scitotenv.2024.171174

Science of the Total Environment 923 (2024) 171174

Contents lists available at ScienceDirect

Science of the Total Environment

journal homepage: www.elsevier.com/locate/scitotenv

Contrasting physiological strategies explain heterogeneous responses to severe drought conditions within local populations of a widespread conifer

Claire Depardieu [a,b,c,*], Patrick Lenz [a,d,1], Joelle Marion [e,1], Simon Nadeau [a,d], Martin P. Girardin [c,f,g], William Marchand [c,f,g], Christian Bégin [e], Kerstin Treydte [h], Arthur Gessler [h,i], Jean Bousquet [a,b], Martine M. Savard [e], Nathalie Isabel [a,c]

[a] Canada Research Chair in Forest Genomics, Institute for Systems and Integrative Biology, Université Laval, Québec, QC G1V 0A6, Canada
[b] Forest Research Centre, Département des sciences du bois et de la forêt, Université Laval, Québec, QC G1V 0A6, Canada
[c] Natural Ressources Canada, Canadian Forest Service, Laurentian Forestry Centre, 1055 rue du P.E.P.S., P.O. Box 10380, Stn. Sainte-Foy, Québec, QC G1V 4C7, Canada
[d] Natural Resources Canada, Canadian Forest Service, Canadian Wood Fibre Centre, 1055 rue du P.E.P.S., P.O. Box 10380, Stn. Sainte-Foy, Québec, QC G1V 4C7, Canada
[e] Geological Survey of Canada, Natural Resources Canada, 490 rue de la Couronne, Québec, QC G1K 9A9, Canada
[f] Centre d'étude de la forêt, Université du Québec à Montréal, C.P. 8888, Succ. Centre-ville, Montréal, QC H3C 3P8, Canada
[g] Forest Research Institute, Université du Québec en Abitibi-Témiscamingue, 445 boul. de l'Université, Rouyn-Noranda, QC J9X 5E4, Canada
[h] Forest Dynamics, Swiss Federal Institute for Forest, Snow and Landscape Research WSL, Birmensdorf, Switzerland
[i] Institute of Terrestrial Ecosystems, ETH Zurich, Zurich, Switzerland

HIGHLIGHTS

- Drought episodes impact negatively white spruce growth in North America.
- A multi-proxy approach was used to assess the intraspecific genetic variation in drought response.
- A reduction of stomatal conductance explained the increase in water-use efficiency of trees under drought conditions.
- Different water-use strategies were observed among trees within populations.
- Trees with higher drought-resilient growth capacity restored water efficiency more effectively.

GRAPHICAL ABSTRACT

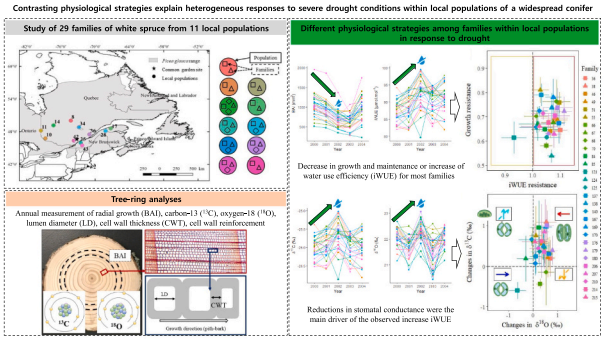

ARTICLE INFO

Editor: Elena Paoletti

Keywords:
Tree rings
Common garden

ABSTRACT

Understanding how trees prioritize carbon gain at the cost of drought vulnerability under severe drought conditions is crucial for predicting which genetic groups and individuals will be resilient to future climate conditions. In this study, we investigated variations in growth, tree-ring anatomy as well as carbon and oxygen isotope ratios to assess the sensitivity and the xylem formation process in response to an episode of severe drought in 29

* Corresponding author at: Canada Research Chair in Forest Genomics, Institute for Systems and Integrative Biology, Université Laval, Québec, QC G1V 0A6, Canada.
E-mail address: claire-paulette.depardieu.1@ulaval.ca (C. Depardieu).
[1] These authors contributed equally to this work.

https://doi.org/10.1016/j.scitotenv.2024.171174
Received 23 October 2023; Received in revised form 12 January 2024; Accepted 20 February 2024
Available online 23 February 2024

White spruce
Intraspecific variation
Water-use efficiency
Drought tolerance

mature white spruce (*Picea glauca* [Moench] Voss) families grown in a common garden trial. During the drought episode, the majority of families displayed decreased growth and exhibited either sustained or increased intrinsic water-use efficiency (iWUE), which was largely influenced by reduced stomatal conductance as revealed by the dual carbon-oxygen isotope approach. Different water-use strategies were detected within white spruce populations in response to drought conditions. Our results revealed intraspecific variation in the prevailing physiological mechanisms underlying drought response within and among populations of *Picea glauca*. The presence of different genetic groups reflecting diverse water-use strategies within this largely-distributed conifer is likely to lessen the negative effects of drought and decrease the overall forest ecosystems' sensitivity to it.

1. Introduction

Acute and chronic droughts induced by climate change are affecting more frequently terrestrial ecosystems, with a strong impact on temperate and boreal forests (IPCC, 2021; Reich et al., 2018; Vicente-Serrano et al., 2020). In such conditions, tree resilience, which refers to the capacity to withstand and recover from environmental disturbance, becomes increasingly critical in determining their long-term viability and productivity (Ingrisch and Bahn, 2018; Lloret et al., 2011). While this topic has received increased attention recently (Gessler et al., 2018; Nikinmaa et al., 2020), the exact physiological mechanisms enabling trees to resist and recover from severe droughts still need to be better comprehended (Brodribb et al., 2020). At issue is the rarity of studies about multi-scale physiological effects from drought episodes as well as the challenges caused by the multiple facets of water stresses (e.g., timing, duration, severity, frequency), which can affect tree resilience (Aldea et al., 2022; Gessler et al., 2020; Ruehr et al., 2019). In this context, the need for thorough investigations of tree resilience in the context of forests and ecosystems facing ongoing climate change remains critical (Ibáñez et al., 2019).

Past research indicated that hydraulic failure and carbon starvation are the two main physiological processes involved in trees' response to drought (Hammond et al., 2019; McDowell et al., 2008). Hydraulic failure, which is induced by limited soil water availability and a high evaporative demand, generally translates into loss of hydraulic contact between soil and roots (Carminati and Javaux, 2020), xylem cavitation, loss of xylem hydraulic conductance and lethal tissue dehydration (Sevanto et al., 2014). Carbon starvation during drought occurs when water scarcity limits the plant's ability to photosynthesize, leading to reduced carbon assimilation and subsequently affecting crucial physiological processes such as growth and energy production (McDowell and Sevanto, 2010). Both carbon deprivation and water loss exert significant impacts on tree vitality, and recent studies converged to indicate hydraulic failure as the main cause of drought-induced tree mortality (Adams et al., 2017; Arend et al., 2021). Previous studies reported that post-drought recovery is no longer possible once the water status has exceeded thresholds of hydraulic impairment due to embolism, confirming the pivotal role of water relations in governing drought response (Brodribb and Cochard, 2009; Choat et al., 2018). Although the capacity to recover physiological function following drought represents a key dimension of tree resilience (Ingrisch and Bahn, 2018), post-drought dynamics and the interaction of carbon and water relations are still poorly understood in woody plants (Munson et al., 2021; Ruehr et al., 2019).

The intrinsic water-use efficiency, that is, the amount of carbon required per unit of water lost, is one major metric to assess drought adaptation in trees (iWUE, Guy and Holowachuk, 2001). Long-term and annual-based changes of iWUE can be inferred by tree-ring records, given that the isotopic discrimination against ^{13}C in leaves (which in turn depends on both determinants of iWUE, stomatal conductance (g_s) and net photosynthetic CO_2 assimilation rate (A) (Farquhar et al., 1982) is reflected in the stable carbon isotope ratio in wood. Thus, iWUE estimated from $\delta^{13}C$ wood sample values represents an integrated measure of plant physiological properties during carbon fixation (Farquhar and Richards, 1984; Farquhar et al., 1982). Although informative, the use of $\delta^{13}C$ alone remains insufficient to determine the source of iWUE variation, i.e., differences in g_s and-or A (Farquhar and Richards, 1984). The dual-isotope approach, where both $\delta^{18}O$ and $\delta^{13}C$ variations in tree rings are analyzed, is a powerful tool to discriminate between water and carbon limitations under drought conditions, given that $\delta^{18}O$ values share a dependence on stomatal conductance with plant $\delta^{13}C$, but remain unaffected by changes in photosynthesis (Scheidegger et al., 2000). Various studies used this approach to better understand the physiological processes involved in growth response to severe droughts (Isaac-Renton et al., 2018) and drought-induced tree dieback (Puchi et al., 2021; Voltas et al., 2013; Wang et al., 2021). A recent conceptual model based on long-term synchronic assessments of growth pattern and dual-isotope information suggests that tree mortality is induced mainly by carbon starvation for trees exhibiting long-lasting gas exchange and growth decline, whereas hydraulic failure would be the main cause of tree death when rapid or no decline of both stomatal conductance and growth prior to death is observed (Gessler et al., 2018). While some empirical observations agree with the predictions of this model (Voelker et al., 2019), other studies suggest that hydraulic failure is a universal component of the physiological processes that precede tree death (Nolan et al., 2021). Given that recovery emerges as a more dependable predictor of mortality than growth-based resistance in certain conifer species (DeSoto et al., 2020), further research appears essential to enhance our understanding of the various tree recovery strategies following severe drought.

Intraspecific genetic variation in drought response is a key determinant of the persistence of tree species in the face of climate change, as it allows for natural selection in the wild but also, it enables the selection of individuals, families or populations to increase drought resilience in tree breeding programs (Laverdière et al., 2022). In coniferous species, numerous studies based on tree-ring data from common garden experiments have revealed the presence of adaptive genetic variation in growth response to severe drought (George et al., 2019; Schueler et al., 2021; Zas et al., 2020), resource use efficiency and photosynthetic rates (Benomar et al., 2016; Isaac-Renton et al., 2018; Zhang and Cregg, 1996), and wood anatomical features (Depardieu et al., 2020). Genome-wide associations or candidate gene approaches revealed a genetic basis for these different types of features, thus of potential usefulness in breeding and selection applications (Housset et al., 2018; De La Torre et al., 2022; Depardieu et al., 2021). Despite this knowledge, traits related to drought sensitivity or tolerance at the individual or family level are still poorly documented, and their potential role in differential genetic adaptation within populations of single species remains to be explored.

White spruce (*Picea glauca* (Moench) Voss) is one of the most widespread conifer species of the temperate and boreal forests of North America, and it generally exhibits high genetic variation within and among populations in growth, wood quality and adaptive capacity (Depardieu et al., 2020; Hassegawa et al., 2020; Li et al., 1993, 1997; Royer-Tardif et al., 2021). Previous studies identified that white spruce's growth was sensitive to warming and increased drought frequency expected under climate change projections (Lapenis et al., 2022; Mirabel et al., 2023; Peng et al., 2011; Sang et al., 2019). A recent report highlighted a low stomatal response to drought among provenances collected across Canada, alongside similar growth resilience across the studied

provenances (Sinclair, 2019). Similar limited potential for other key physiological parameters to cope with temperature warming was also observed (Benomar et al., 2018). In the context of more frequent droughts under a warming and more unstable climate, these findings suggest an inevitable decline owing to the populations' limited adaptive capacity, on average (Hogg et al., 2017). However, our earlier study in eastern Canada revealed a distinct trend in local genetic adaptation: populations originating from drier climates exhibited greater resilience to severe drought compared to those from more humid regions (Depardieu et al., 2020). The severe drought episode of 2001–2002, led to a significant decrease in tree growth, ranging from 15 to 21 % (Depardieu et al., 2020). Yet, following the drought, noticeable growth recovery was observed in trees as early as 2003. The tested populations displayed variations in recovery and growth resilience, both of which were heritable traits showing substantial genetic diversity among provenances and among families within these provenances. In this study, to further gain insight into the physiological processes underlying variation in drought resilience in white spruce, we carried out a multi-proxy and retrospective analysis of growth, wood anatomical traits, and tree-ring stable isotopes in response to the major drought episode of 2001–2002 in eastern Canada. By studying 29 spruce families in conjunction with this integrative approach, we aimed to (1) identify the physiological mechanisms (i.e., the control of stomata aperture and photosynthesis) involved in response, recovery, and resilience to severe drought (Fig. 1), (2) determine which of carbon starvation or water stress is the dominant response to drought stress within and among white spruce provenances, and (3) analyze the selection potential for high iWUE while maintaining growth productivity in this species.

2. Material and methods

2.1. Experimental design

The common garden experiment used in this study was established by the Canadian Forest Service in 1979 near the locality of Mastigouche, Quebec, Canada (Lat. 46°38′ N, Long. 73°13′ W, elevation 230 m). The experiment utilized 4-year-old open-pollinated seedlings sourced from 43 white spruce provenances, representing the geographic locations where tree seeds were collected back in the 1960s (Figure SM1 in Methods 1; Table S1). These seedlings were planted at a spacing of 1.2 m, with 2.4 m between each row. The experimental design consisted of a randomized complete block design. To assess the extent of genetic variability in growth and physiological resistance in this study, we selected eleven white spruce populations growing in the trial that exhibited contrasting growth responses to the 2001–2002 severe drought episode in eastern Canada (Methods S1). Within each population, 2 to 4 distinct groups of trees, with each group corresponding to an open-pollinated family thus with a mother tree in common (half-sib family), were selected for phenotypic and genetic analyzes based on their resilience indices (Figure SM1C-D in Methods S1). This selection aimed to maximize differences between families, ensuring a representative sample that reflected the observed genetic variation in the complete dataset. The seed sources and half-sib families studied here were distributed along gradients of soil moisture and mean annual temperature in the province of Québec, Canada (Table S1). A total of 123 trees from 29 half-sib families were sampled and analyzed for growth, isotopic values, and wood anatomy (Table S2). Families were each represented by 3 to 9 trees.

2.2. Tree growth and wood anatomy

Long-term growth traits such as tree height (H) and stem diameter at breast height (DBH) were measured at 38 years of age during summer 2017. Xylem traits were measured from a 12-mm wood increment core extracted around breast height from each tree in 2006 and further processed as previously described (see Beaulieu et al., 2020). Wood traits were obtained by combining image analysis, x-ray densitometry and diffractometry at the FPInnovations facilities (Vancouver, BC, Canada) using the SilviScan technology. The ring width and simple cell-wall thickness (WT) were measured at consecutive radial intervals of 25 μm. Cross-dating quality was validated using the program COFECHA, by moving correlations between individual series and a reference mean

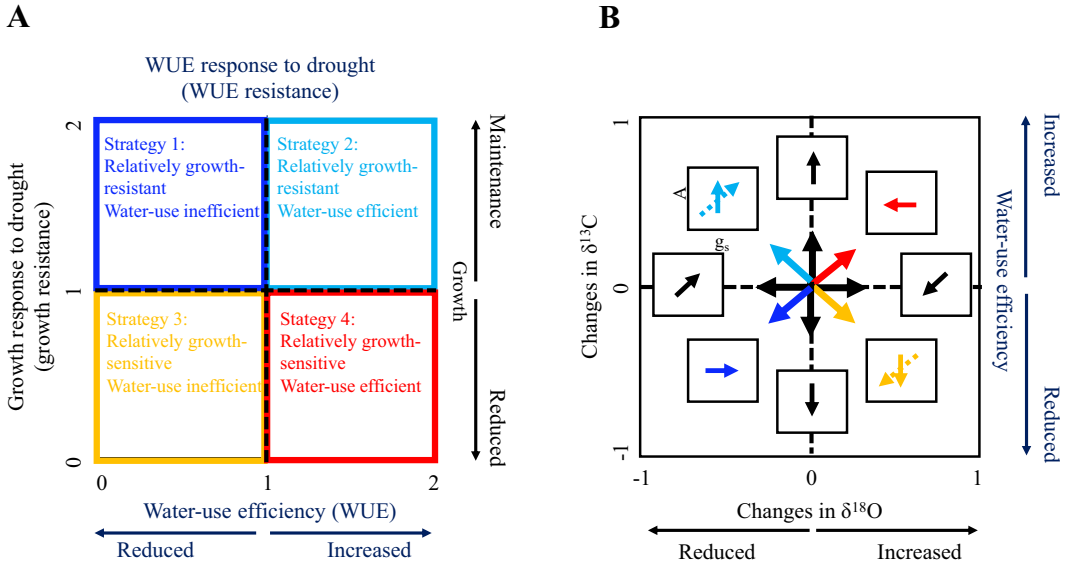

Fig. 1. Tree-ring isotope-based conceptual framework used in this study. (A) Conceptual application of the model proposed by Gessler et al. (2018) and adapted for white spruce trees, showing growth and isotope composition ratios between non-drought and drought years. The growth ratios are plotted against the $\delta^{13}C$ ratio ($\delta^{13}C$ resistance) resulting in four quadrants indicating four hypothesized patterns, that is. a maintained growth and decreased water-use efficiency (WUE) (Strategy 1: blue square), maintained growth and increased WUE (Strategy 2: turquoise square), a reduced growth and decreased WUE (Strategy 3: orange square), and a reduced growth and increased intrinsic water-use efficiency (Strategy 4: red square). (B) Conceptual application of the Scheidegger/Grams models (adapted from Scheidegger et al., 2000). Changes in $\delta^{13}C$ response to environmental fluctuations are plotted against the $\delta^{18}O$ changes. Small inserts indicate the interpretation of each $\delta^{13}C$–$\delta^{18}O$ combination, in terms of changes in net photosynthesis (A) and stomatal conductance (g_s). The alternative interpretation for the orange and light blue scenarios are indicated by dashed lines (Grams et al., 2007).

series or site chronology (Holmes, 1983). Ring-width series were converted to ring-area series (basal area increments, BAI) based on the distance between the innermost measured ring and the pith of the tree (dplR R package; Bunn, 2008). The wood resistance (WR), that is, the latewood proportion of ring width, was calculated for each ring and expressed in percentage. In conifers, latewood was found more vulnerable to embolism than earlywood, meaning that a higher proportion of latewood would likely lead to an increase in vulnerability to embolism (Martinez-Meier et al., 2008). The cell wall reinforcement (CWR), a measure reflecting xylem resistance to drought-induced embolism (Hacke et al., 2001), was calculated as the ratio of tracheid wall to lumen diameter, squared, in both radial and tangential directions. Lumen diameter (LD) was estimated using LD = TD - CWT, with TD indicating tracheid diameter and CWT representing cell wall thickness (CWT = 2*WT), assessed radially and tangentially. The average lumen diameter and cell wall reinforcement were subsequently calculated as the mean values derived from radial and tangential parameters.

Principal component analysis (PCA) was conducted to select the most representative growth and anatomical traits, given that the measured traits can be highly correlated. The analysis was based on a correlation matrix of all the measured and derived traits, and considering the 2000–2004 period. The overall significance of the PCA, of each PC axis and of the contribution of each trait to the significant axes was determined using the PCAtest R package (Camargo, 2022). PCA plot was then generated to display the similarities among the tested traits.

2.3. Isotope analyzes

2.3.1. Pilot study: determining the most suitable methodology for isotopic measurements

Given the efficacy of whole-wood samples as substitutes for cellulose in assessing the influences of climate variation on tree-ring $\delta^{13}C$ and $\delta^{18}O$ values in short-term ecophysiological and dendrochronological studies (Isaac-Renton et al., 2018; Weigt et al., 2015), we conducted a pilot study to ascertain if whole wood was adequate for isotopic analysis of white spruce samples, which would avoid the need for cumbersome cellulose extractions on large number of samples (see Methods S2). Strong correlations of isotope measurements between whole wood and cellulose were observed ($r = 0.96$ for $\delta^{18}O$ and 0.97 for $\delta^{13}C$; Fig. MS2 in Methods S2), thus eliminating the need for cellulose extraction in our study, and validating the direct assessment of isotopic values from whole wood samples.

2.3.2. Isotope measurements

Two 5 mm cores were taken from each tree at breast height in the south and north directions of the stems at the end of the 2017 and 2018 growing seasons. Annual-based rings were separated from both wood cores for each tree and cut into thin slices using a razor blade and a binocular (Methods S3). Thin wood slices were then ground using the RETSCH Mixer Mill MM 400 (Fisher Scientific, Canada). Finally, wood samples were weighed into tin (carbon) or silver (oxygen) capsules for elemental analyses and mass spectrometry.

Individual $\delta^{13}C$ and $\delta^{18}O$ measurements were performed on bulk-wood with an annual resolution for the years 2000–2004. This period included the major 2001–2002 drought event (Wheaton et al., 2008; Fig. S1) where white spruce populations differed in their growth responses (see Depardieu et al., 2020). Isotopic values were measured on a total of 1230 whole wood samples at the Delta-Lab of the Geological Survey of Canada (Quebec City, QC, Canada). Homogenized wood powder samples were analyzed using an elemental analyzer (Costech, Valencia, CA, USA) for $\delta^{13}C$ values and a thermal conversion elemental analyzer (Thermo Finnigan, Bremen, Germany) for $\delta^{18}O$ measurements, coupled to an isotope ratio mass spectrometer (Delta Plus XL; Thermo Finnigan, Bremen, Germany). Calibration for $\delta^{13}C$ and $\delta^{18}O$ results was done based on international (IAEA-CO-1, LSVEC, IAEA-CH-6 for $\delta^{13}C$ and IAEA-602, IAEA-CH-6, USGS-56 for δ18O), and in-house standards and referenced to VPDB for $\delta^{13}C$ and to VSMOW for $\delta^{18}O$. The analytic precision is of 0.1 and 0.2 ‰, respectively.

The ratios of the heavier to lighter isotopes (R) are reported using the 'δ' notation in peer mil (‰) as follow:

$$R_{isotope} = \left[\left(R_{sample}/R_{reference}\right) - 1\right] 1000 \quad (1)$$

where R_{sample} and $R_{reference}$ are the isotopic ratios of the sample and the international standard, respectively.

2.3.3. iWUE inferred from carbon isotope discrimination

We calculated several proxies reflecting changes in water use, such as the carbon isotope ratio ($\delta^{13}C$) in tree rings, the carbon isotope discrimination $\Delta^{13}C$ and the intrinsic water-use efficiency iWUE. The $\Delta^{13}C$ is generally used as a reliable proxy for iWUE of photosynthesis (Kruse et al., 2012), and is here examined in tree-ring wood samples to get insights into changes in gas exchange physiology. The $\Delta^{13}C$ values were calculated with the following equation:

$$\Delta^{13}C = \left(\delta^{13}C_{atmo} - \delta^{13}C\right)/\left(1 + \delta^{13}C/1000\right) \quad (2)$$

where $\Delta^{13}C$ is the carbon isotope discrimination (‰), $\delta^{13}C_{atmo}$ is the isotopic value of atmospheric CO_2 and $\delta^{13}C$ is the isotopic value of the whole wood formed that year (Fig. S2). The $\Delta^{13}C$ was calculated using annual estimates of $\delta^{13}C_{atmo}$ obtained from the literature (see Graven et al., 2017).

To gain further insights into changes in gas exchange physiology over time, we calculated the ratio of intercellular to atmospheric [CO_2] (c_i/c_a) from the $\Delta^{13}C$ values (Farquhar et al., 1982):

$$c_i/c_a = \left(\Delta^{13}C - a\right)/(b - a) \quad (3)$$

where a is the fractionation associated with CO_2 diffusion through the stomata ($a = 4.4$ ‰), b is the fractionation during carboxylation ($b = 27$ ‰). The c_i value was calculated using the growing season c_a (i.e. the average of monthly-based values, from May to October included), which was obtained from direct measurements of atmospheric CO_2 levels recorded at Mauna Loa, Hawaii (see Keeling et al., 2009; https://cdiac.ess-dive.lbl.gov/trends/co2/sio-mlo.html).

To further examine changes in the balance between photosynthesis (A) and stomatal conductance (g_s) over time, we also calculated the intrinsic water-use efficiency (iWUE) with the following equation (Farquhar et al., 1982):

$$iWUE = A/g_s = (c_a - c_i)/1.6 \quad (4)$$

2.3.4. Oxygen isotope analyses

Oxygen isotope discrimination in tree rings ($\Delta^{18}O_{ring}$) was calculated according to Cheesman and Cernusak (2017):

$$\Delta 18O = \frac{\delta 18O - \delta 18OPrec}{1 + \left(\frac{\delta 18OPrec}{1000}\right)} \quad (5)$$

where $\delta^{18}O$ is the oxygen isotope composition measured in tree rings, while $\delta^{18}O_{Prec}$ is the $\delta^{18}O$ of precipitation (assumed to equal source water), which we estimated as described below. Given that the plots were spatially collocated and trees were of the same age, we assumed that the source water $\delta^{18}O_{prec}$ was similar for all the sampled trees.

We estimated annual values of precipitation $\delta^{18}O$ ($\delta^{18}O_{Prec}$) at the common garden site as previously described by Barbour et al. (2001), by using the following equation:

$$\delta^{18}O_{Prec} = 0.52\,Ta - 0.006\,Ta^2 + 2.42\,Pa - 1.43\,Pa^2 - 0.046\sqrt{E} - 13 \quad (6)$$

where Ta, Pa and E are the annual temperature, precipitation (this latter expressed in m) and elevation (m asl), respectively. The elevation of the Mastigouche common garden site is 230 m.

2.4. Quantification of drought response of growth, wood anatomy and isotopic values

Components of tree resilience such as resistance (Rs), recovery (Rc) and resilience (Rl) were calculated based on tree growth rates, as previously described by Lloret et al. (2011). Resistance (Rs) describes a tree's ability to absorb changes in radial growth due to drought and was calculated as the ratio of BAI during the drought event to BAI before the event. Recovery (Rc) represents the capacity of tree growth to rebound after the drought and was calculated as the ratio of BAI after the event to BAI during the event. Lastly, resilience (Rl) indicates the tree's ability to return to pre-drought growth rates and was calculated by dividing post-drought BAI values by pre-drought BAI values. Those three resilience indices (Rs, Rc and Rl) were also calculated for the water-use efficiency (iWUE), growth and wood anatomical traits to further quantify their response to the severe 2001–2002 drought episode. Rs, Rc and Rl were calculated considering a 1-year period drought event (2002; see Depardieu et al., 2020 for details), while two consecutive years defined the pre-drought (2000−2001) and the post-drought (2003–2004) periods. Concomitant changes of BAI and iWUE were interpreted according to the conceptual model proposed by Gessler et al. (2018) (Fig. 1A).

The mean $\delta^{13}C$ and $\delta^{18}O$ changes between drought and pre-drought years, which are reflecting the isotopic responses to drought, were calculated as Rs_$\delta^{13}C$ = $\delta^{13}C$drought - $\delta^{13}C$pre-drought and Rs_$\delta^{18}O$ = $\delta^{18}O$drought - $\delta^{18}O$pre-drought, respectively. Similarly, isotopic changes during the recovery phase were calculated as Rc_$\delta^{13}C$ = $\delta^{13}C$post-drought - $\delta^{13}C$drought and Rc_$\delta^{18}O$ = $\delta^{18}O$post-drought - $\delta^{18}O$drought. Isotopic variation between pre-drought and post-drought years were also quantified and defined as Rl_ $\delta^{13}C$ = $\delta^{13}C$post-drought - $\delta^{13}C$pre-drought and Rl_$\delta^{18}O$ = $\delta^{18}O$post-drought - $\delta^{18}O$pre-drought. Isotope reaction patterns between two time periods were then interpreted into changes of g_s and A, according to the conceptual models developed by Scheidegger and Grams (Grams et al., 2007; Scheidegger et al., 2000; Fig. 2B). The means and standard errors for comparisons of resilience components among families, and the ANOVA outcomes for family effects are presented in Table S6.

To test whether drought had a consistent effect on the isotope ratios for each white spruce family, one-sample *t*-tests were used to determine whether $\delta^{13}C$ and $\delta^{18}O$ response, recovery, and resilience differed significantly from zero. The same methodology was applied for the three resilience components calculated from iWUE and BAI, and considering a baseline mean of 1 for the t-tests. A significant t-test with a family mean >1 would indicate an increase in water-use efficiency or radial growth, while the opposite would apply if the mean was <1. To address the plot effect and prevent pseudo-replication, we averaged values within each plot before conducting t-tests. To reduce potential biases in our recovery findings due to autocorrelation structures, we analyzed the relationship between growth resilience indices and individual tree autocorrelation coefficients (using the acf function in the stats R package). This precaution was taken because stronger autocorrelation might create a lasting impact, potentially obscuring our ability to detect legacy effects after rare weather events (Klesse et al., 2023). However, upon thorough review, we confirmed that our results remained unaffected by this specific autocorrelation-related bias, as we found no significant correlation between the resilience indices and the autocorrelation coefficients.

2.5. Quantitative genetic analyses

The effects of genetics, time, and drought were tested by fitting an individual-tree linear mixed model using the realized additive genomic

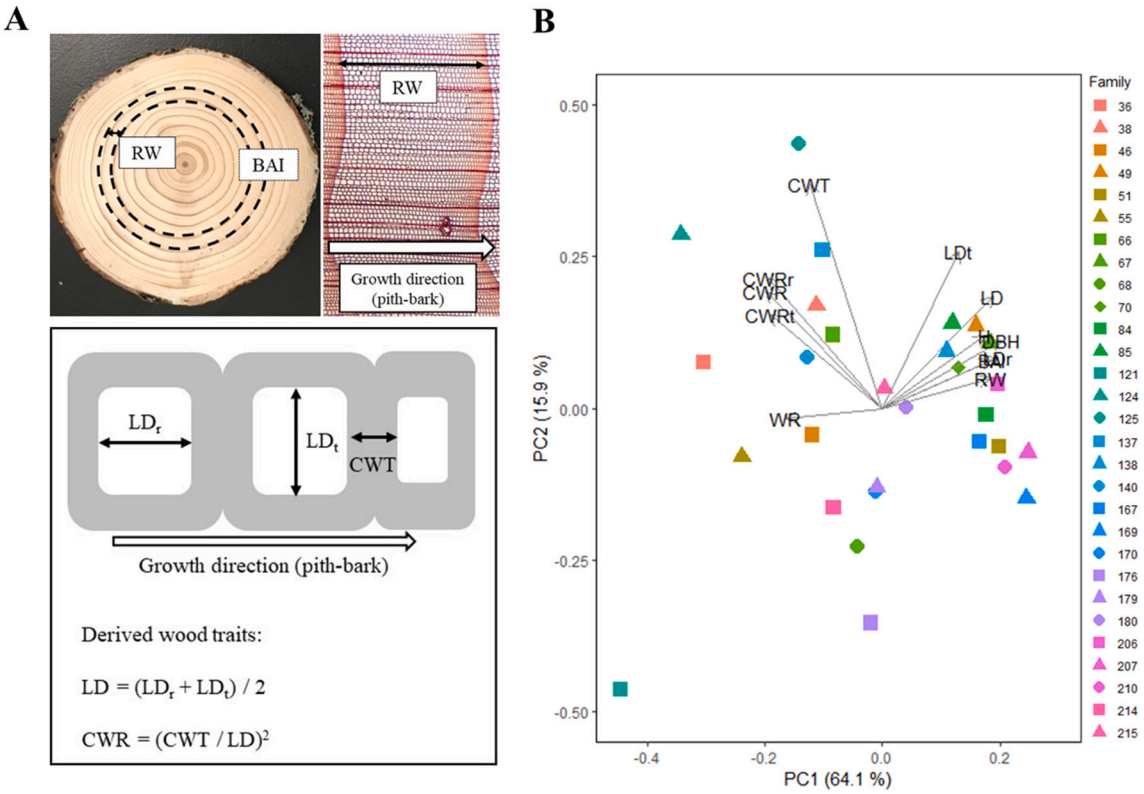

Fig. 2. Tree-ring traits analyzed in this study. (A) Cross-section of a white spruce trunk (left), microscopic wood anatomy (center), and calculation of derived variables (right). Photo credit: Martine Blais (Natural Resources Canada) and Claire Depardieu (Univ. Laval). (B) Selection of tree-ring traits as representative for growth-related and hydraulic-related groups. Scatterplots of the first two principal components PC1 and PC2 calculated based on provenance (left) and family (right) means of growth indices and wood anatomy. Abbreviations are as follows: RW: ring width; BAI: basal area increment; LDr: radial and tangential lumen diameter, respectively; CWT: cell wall thickness; CWRr and CWRt: radial and tangential cell wall reinforcement, respectively; H: height; DBH: diameter at breast height; WR: latewood percentage of ring width, or wood resistance.

relationship matrix (***G***-matrix) using ASReml-R v.4.1 ("GBLUP model"; Butler et al., 2017; see Tables S3 and S4). The ***G***-matrix was computed from 6140 single nucleotide polymorphism markers (Depardieu et al., 2021) using the 'A.mat' function of the RRBLUP R package (Endelman and Jannink, 2012) with the default options. The following individual-tree linear mixed models were fitted:

$$\boldsymbol{y} = \boldsymbol{X\beta} + \boldsymbol{Z_1 p}(\boldsymbol{year}) + \boldsymbol{Z_2 a}(\boldsymbol{year}) + \boldsymbol{e} \quad (7)$$

where $\boldsymbol{y}$ is the phenotypic observed values; $\boldsymbol{\beta}$ is a vector of fixed effects including the overall mean, the year, and the block within year effects. The plot effect was nested within year and was defined as $\boldsymbol{p}(\boldsymbol{year}) \sim N(\boldsymbol{0}, \boldsymbol{V_p} \otimes \boldsymbol{I_p})$. The random additive genetic effect was nested within year and defined using the ***G***-matrix as $\boldsymbol{a}(\boldsymbol{year}) \sim N(\boldsymbol{0}, \boldsymbol{V_a} \otimes \boldsymbol{G})$. The $\boldsymbol{X}$ and $\boldsymbol{Z}$ matrices are incidence matrices of their corresponding effects, $\boldsymbol{I_p}$ is an identity matrix of dimension p (107 plots), and the symbol $\otimes$ is the Kronecker product. Given the repeated measures on the same increment core, the error term was assumed to be $\boldsymbol{e} \sim N(\boldsymbol{0}, \boldsymbol{I_l} \otimes \boldsymbol{R})$ where $\boldsymbol{I_l}$ is an identity matrix of dimension l (123 trees), $\boldsymbol{R}$ represents a first-order heterogeneous autoregressive correlation structure (AR1H) on time of dimension 5 × 5 years. Similarly, the matrices $\boldsymbol{V_p}$ and $\boldsymbol{V_a}$ represented 5 × 5 variance-covariance matrices defined by the variances within years, and the correlation of variances across years for the plot and additive genetic effects, respectively. For these two matrices, we tested various variance-covariance structures, namely the identity (ID), diagonal (DIAG), compound symmetry (CS), uniform heterogeneous (CORH), and the first-order heterogeneous autoregressive (AR1H). These variance-covariance structure can be represented as follow:

$$ID = \begin{bmatrix} \sigma^2 & \cdots & 0 \\ \vdots & \ddots & \vdots \\ 0 & \cdots & \sigma^2 \end{bmatrix}; DIAG = \begin{bmatrix} \sigma_1^2 & \cdots & 0 \\ \vdots & \ddots & \vdots \\ 0 & \cdots & \sigma_2^2 \end{bmatrix};$$

$$CS = \begin{bmatrix} \sigma^2 & \cdots & \rho \\ \vdots & \ddots & \vdots \\ \rho & \cdots & \sigma^2 \end{bmatrix}; CORH = \begin{bmatrix} \sigma_1^2 & \cdots & \rho \\ \vdots & \ddots & \vdots \\ \rho & \cdots & \sigma_5^2 \end{bmatrix}$$

$$AR1H = \begin{bmatrix} \sigma_1^2 & \cdots & \rho^5 \\ \vdots & \ddots & \vdots \\ \rho^5 & \cdots & \sigma_5^2 \end{bmatrix}.$$

The ID and CS structure fitted a uniform within-year variance σ^2. The DIAG, CORH, and AR1H fitted heterogeneous within-year variances from year 2000 (σ_1^2) to year 2004 (σ_5^2). The CS and CORH fitted a uniform correlation across years ρ, while the AR1H fitted a first-order autoregressive correlation. The best model was chosen based on the Aikaike information criterion (AIC) (Tables S3 and S4). Since resilience components (e.g., resistance, recovery, and resilience traits) were not analyzed for distinct years, the plot, additive genetic, and error terms were specified as $\boldsymbol{p} \sim N\left(\boldsymbol{0}, \sigma_p^2 \boldsymbol{I_p}\right)$, $\boldsymbol{a} \sim N(\boldsymbol{0}, \sigma_a^2 \boldsymbol{G})$, and $\boldsymbol{e} \sim N(\boldsymbol{0}, \sigma_e^2 \boldsymbol{I_e})$, respectively.

The individual narrow-sense heritability (h^2) estimates, that is, the proportion of phenotypic variance that is accounted for by the additive genetic variance, were calculated as:

$$h2 = \frac{\overline{\sigma_a^2}}{\overline{\sigma_p^2} + \overline{\sigma_a^2} + \overline{\sigma_e^2}} \quad (8)$$

where $\overline{\sigma_p^2}$, $\overline{\sigma_a^2}$, and $\overline{\sigma_e^2}$ are the average plot, additive genetic, and residual variances across years, respectively. Standard errors of heritability estimates were obtained using the delta method (*vpredict* function from the ASREML-R package version 4.1). Given the relatively small heritability estimates and nonsignificant additive genetic variances found for most of the resilience components, only traits with significant heritability estimates are presented in the results.

Genetic and phenotypic correlations were estimated using a bivariate model (for details see Methods S4), using mean phenotypic values for the 2000–2004 period. Genetic correlations between traits are solely contingent on the correlation of additive genetic effects, whereas phenotypic relationships hinge on both additive genetic and environmental effects. Correlations were visualized by generating matrices using the R corrplot package (Wei and Simko, 2017).

All data analyses were performed using Rstudio (R Core Team, 2022). In all cases, the normality of the data was previously checked and either square root, logarithmic, or logit transformations were applied whenever necessary. The quality of fit was assessed using residual distribution plots obtained using qqnorm plots of standardized residuals against quantiles of standard normal. Model parameters were estimated with the restricted maximum likelihood method (REML).

3. Results

3.1. Selection of anatomical and growth-related traits for detailed analysis

This study first evaluated growth-related traits such as basal area increment (BAI), ring width (RW), height (H), and diameter at breast height (DBH) (see Table 1 for detailed abbreviations; Fig. 2A). Additionally, we assessed wood anatomical traits such as wood resistance (WR), wood density (WD), cell wall thickness (CWT), along with the radial, tangential, and mean components of cell wall reinforcement (CWR) and lumen diameter (LD) (Table 1; Fig. 2A). The PCA revealed that the principal component PC1 was significant and accounted for 64.1 % of the total variation, while PC2 accounted for 15.9 % of the total variation (Fig. 2B). Three groups were identified, with the first group gathering growth-related (BAI, RW) and hydraulic-related (LD, LDr) traits, a second group containing the more long-term cumulative growth indicators such H and DBH, and a third group containing radial, tangential, and mean components of cell wall reinforcement (CWRt, CWRr, and CWR) and CWT (Fig. 2B). Upon these findings, we identified basal area increment (BAI) and height (H) as well representative of spruce growth, and we considered wood resistance (WR), radial cell wall reinforcement, and lumen diameter (CWRr and LDr) as deemed relevant hydraulic-related traits. CWRr and LDr were chosen considering their marginally higher heritability than CWR and LD (Depardieu et al., 2020). As the only trait linking hydraulics with carbon use, CWT was also retained for further analyses.

3.2. Annual variation of representative wood traits and stable isotopes

Family-averaged annual changes in BAI, isotopic parameters ($\delta^{18}O$, $\delta^{13}C$, and iWUE), and representative wood characteristics (WR, CWRr, LDr, and CWT) are presented in Fig. 3. The summer drought conditions in 2002 (Fig. S1) resulted in a decrease in radial growth for all families in 2002 (Fig. 3A), which was accompanied by a reduction of radial lumen diameter (LDr) and increases in radial cell wall reinforcement (CWRr) and latewood percentage (WR; Fig. 3F-H). The iWUE, $\delta^{18}O$, and $\delta^{13}C$ values notably increased in 2002 across the majority of white spruce families (Fig. 3B-D). During the post-drought recovery period in 2003 and 2004, growth resumed its upward trend (Fig. 3A and F), while radial cell wall reinforcement, wood resistance, $\delta^{18}O$, and $\delta^{13}C$ values either decreased or stabilized (Fig. 3G-H and 3C-D, respectively).

3.3. Response, recovery and resilience of white spruce families to drought

The concomitant changes in the growth and water-use efficiency of families on the one hand, and in their carbon and oxygen isotopes on the other, are presented in Fig. 4. Except for four families (68, 121, 169 and 176), all families reduced their growth and maintained or even

Table 1
Overview of the traits analyzed in this study. Trait type, name, and description are reported for the representative measured traits and the calculated tree-ring traits. Basic statistics such as the mean, standard deviation (SD) and the coefficient of variation (CV) are presented below. For traits measured annually, averages were calculated from the average of the trait measured over the 2000–2004 period (that is, BAI, RW, CWT, WD, LDr, CWRr, WR, $\delta^{18}O$, $\delta^{13}C$, and iWUE).

Trait type	Abbreviation	Trait description	Units	Mean	SD	CV
Growth-related	RW	Ring width	mm	2.76	0.72	26.12
	BAI	Basal area increment	mm^2	862.10	401.12	46.53
	H	Height (measured 38 y-o)	cm	1381.14	216.08	15.64
	$BAI_{1999–2017}$	Long-term radial growth performance	mm^2	702.09	349.95	49.84
Wood anatomy	CWT	Cell wall thickness	µm	4.23	0.38	9.02
	WD	Wood density	$kg{\cdot}m^{-3}$	414.06	37.10	8.96
	LDr	Radial lumen diameter	µm	25.90	2.07	8.00
	LDt	Tangential lumen diameter	µm	23.79	1.64	6.90
	LD	Average lumen diameter	µm	24.84	1.60	6.44
	CWRr	Radial cell wall reinforcement	µm	2.79	0.77	27.45
	CWRt	Tangential cell wall reinforcement	µm	3.24	0.75	23.06
	CWR	Average cell wall reinforcement	µm	3.02	0.73	24.10
	WR	Latewood proportion of ring width, or wood resistance	%	0.14	0.04	27.68
Physiology-related	$\delta^{18}O$	Oxygen isotopic ratio	‰	21.93	0.54	2.48
	$\delta^{13}C$	Carbon isotopic ratio	‰	−25.91	0.54	−2.10
	iWUE	Intrinsic water-use efficiency	$\mu mol.mol^{-1}$	90.06	5.90	6.56
Drought response	Rs_BAI	Growth resistance	unitless	0.69	0.10	14.99
	Rc_BAI	Growth recovery	unitless	1.19	0.31	26.18
	Rl_BAI	Growth resilience	unitless	0.82	0.23	28.46
	Rs_CWT	Response of cell wall thickness to drought	unitless	1.02	0.05	5.09
	Rc_CWT	Recovery of cell wall thickness after drought	unitless	1.05	0.06	5.65
	Rl_CWT	Resilience of cell wall thickness	unitless	1.07	0.05	5.08
	Rs_LDr	Response of radial lumen diameter to drought	unitless	0.94	0.04	3.89
	Rc_LDr	Recovery of radial lumen diameter after drought	unitless	1.02	0.04	3.92
	Rl_LDr	Resilience of radial lumen diameter	unitless	0.97	0.04	4.00
	Rs_CWRr	Response of radial cell wall reinforcement to drought	unitless	1.18	0.17	14.61
	Rc_CWRr	Recovery of radial cell wall reinforcement after drought	unitless	1.07	0.16	14.98
	Rl_CWRr	Resilience of radial cell wall reinforcement	unitless	1.23	0.19	15.15
	Rs_WR	Response of wood resistance to drought	unitless	1.70	0.73	43.07
	Rc_WR	Recovery of wood resistance after drought	unitless	1.11	0.49	44.37
	Rl_WR	Resilience of wood resistance	unitless	1.63	0.38	23.17
	Rs_iWUE	Response of intrinsic water-use efficiency to drought	unitless	1.06	0.07	7.11
	Rc_iWUE	Recovery of intrinsic water-use efficiency after drought	unitless	0.98	0.07	6.98
	Rl_iWUE	Resilience of intrinsic water-use efficiency	unitless	1.03	0.05	4.79
Isotopic drought sensitivity	Rs_$\delta^{13}C$	$\delta^{13}C$ changes in response to drought	‰	0.36	0.60	167.15
	Rc_$\delta^{13}C$	$\delta^{13}C$ changes during the recovery period	‰	−0.36	0.54	−150.66
	Rl_$\delta^{13}C$	$\delta^{13}C$ changes between the pre-drought and post-drought periods	‰	0.01	0.39	48,565.69
	Rs_$\delta^{18}O$	$\delta^{18}O$ changes in response to drought	‰	0.45	0.95	209.77
	Rc_$\delta^{18}O$	$\delta^{18}O$ changes during the recovery period	‰	−0.55	0.91	−165.02
	Rl_$\delta^{18}O$	$\delta^{18}O$ changes between the pre-drought and post-drought periods	‰	−0.09	0.65	−749.99

increased their water-use efficiency in response to drought (Fig. 4A; Table S6). Growth resistance was strictly <1 and differed significantly between families (Rs_BAI; Fig. 4A; Tables S4 and S5). All families except 121 had increased mean iWUE values in response to drought, with families 51, 124, 167 and 180 exhibiting consistent increases in iWUE (Table S6). Variation in $\delta^{13}C$ and $\delta^{18}O$ values suggested that for most families, the stress response resulted in a reduction in stomatal conductance g_s, sometimes coupled (families 66, 67, and 121) with a reduction in net assimilation A (Fig. 4B).

After the drought episode, the mean growth recovery was not significantly different from 1 for all families, except for family 68 which had a significantly greater recovery than the other families, and family 215 which exhibited a further growth reduction during the post-stress period (Fig. 4C). Values of iWUE recovery (Rc_iWUE) were particularly low for families 36, 67, 124, and 207 (Fig. 4C; Table S6). An increase in g_s potentially coupled with an increase in A was observed for most families, except for families 170 and 121 (Fig. 4D). Low $\delta^{18}O$ values were consistently observed for families 67, 70, 125, 210 and 214, while families 36, 51, 124, 167, 207 and 214 exhibited a pronounced reduction of $\delta^{13}C$ values (Fig. 4D; Table S6).

Variations in growth resilience were evident across the studied families (Fig. 4E). *t*-tests indicated that seven families exhibited growth resilience values consistently below 1 (specifically families 49, 70, 124, 138, 210, 214, and 215; Fig. 4E and Table S5). A consistent adjustment in water-use efficiency to cope with stress conditions was observed for five families (i.e., 51, 68, 125, 140 and 167) with mean Rl_iWUE values strictly >1 (Fig. 4E; Table S6). With regard to the concurrent variation in $\delta^{13}C$ and $\delta^{18}O$, the family means were dispersed across four scenarios or distinct physiological strategies, as illustrated in Fig. 4F. Variations in iWUE before and after the water stress period for families 51 and 68, showcasing the greatest resilience in growth and water-use efficiency, are attributed to a decrease in stomatal conductance, possibly linked with a decline in net assimilation (Fig. 4E-F). On the contrary, families 124 and 215, which were the least resilient for growth and WUE, showed a physiological balance corresponding to a higher stomatal conductance and/or assimilation in the post-stress period compared to the pre-stress period.

3.4. Genetic parameters and correlations between traits

Both phenotypic and genetic correlations revealed an absence of correlation between water-use efficiency (iWUE) and growth indicators (i.e. BAI, H, and BAI_1999_2017; Fig. 5). However, positive correlations were observed between iWUE and both resistance and resilience components of CWRr and CWT (Fig. 5A and B). Growth resilience (Rl_BAI) was negatively correlated with the two embolism proxies (e.g. CWRr and WR; Fig. 5A and B). Rl_BAI was also negatively associated with CWT. Both phenotypic and genetic correlations revealed that greater growth resilience was associated with a greater ability to modulate their iWUE in response to drought (i.e. higher Rl_iWUE).

Narrow-sense heritability estimates (h^2) were significant for all traits repeated over time, with CWRr and LDr being the most heritable traits

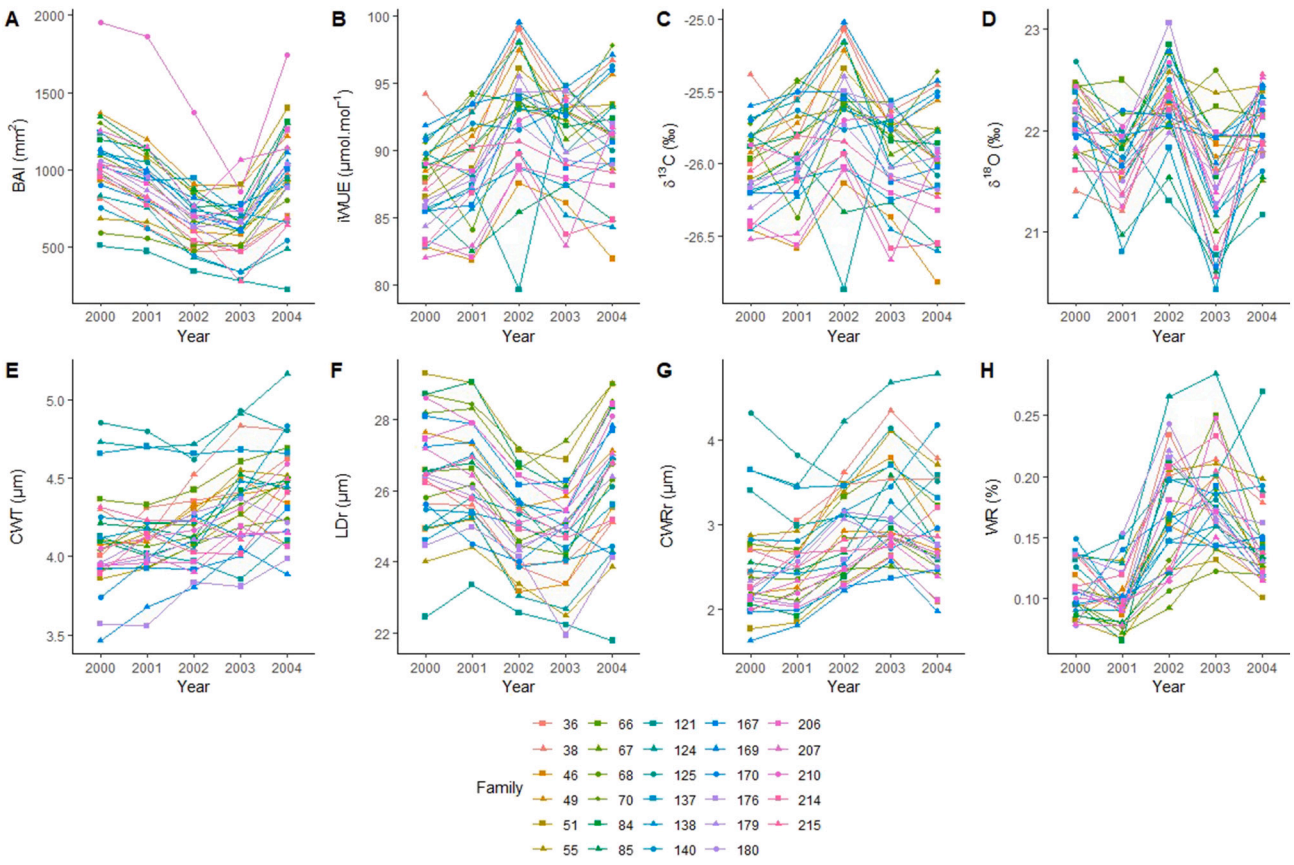

Fig. 3. Temporal trends of families' values for growth, wood anatomy, isotopic values and water-use efficiency for the period 2000–2004. Variation in basal area increment (BAI) is presented in panel A. The water–use efficiency (iWUE), carbon and oxygen isotopic values are presented in panels B—D. The representative wood anatomical traits are the double cell wall thickness (CWT; E), radial lumen diameter (LDr; F), radial cell wall reinforcement (CWRr; G), and wood resistance (WR; H). In this figure, families belonging to the same population have similar color.

($0.77 \leq h^2 \leq 0.79$), followed by iWUE and the three growth resilience components ($0.62 \leq h^2 \leq 0.78$). CWT and $\delta^{18}O$ were the least heritable traits ($h^2 = 0.20$ and $h^2 = 0.25$, respectively; Table 2).

4. Discussion

In this study, we used a multi-parameter approach to analyze the patterns of intraspecific variation of xylem properties, growth-related tree-ring traits and isotopic ratios of 29 open-pollinated white spruce families experiencing a severe drought episode, in order to elucidate the physiological processes underlying drought resilience in a widely distributed conifer species. By relying on the dual isotopic approach, we evaluated whether stomatal or photosynthetic regulation was the primary response to drought stress among families. We report notable variability in the nature and relative contributions of physiological processes involved in the response and recovery to a major drought episode in the studied families. Our study highlights the relevance of analyzing the genetic variation in tree-ring traits related to wood formation and physiology to improve our understanding of resilience to drought in conifers.

4.1. Growth, water-use efficiency and anatomical features in response to severe drought: physiological implications

Through a retrospective analysis of wood traits and isotopic ratios, we showed that drought conditions impacted growth, wood anatomy and the physiological status of white spruce trees (Fig. 3; Fig. S3). Drought conditions caused a drastic reduction in radial growth and lumen diameters, which is usually accompanied by a reduction in hydraulic conductivity and overall water transport in trees, as a response to a decline in turgor (Pellizari et al., 2016; Pittermann et al., 2006). To secure immediate survival during critical drought periods, trees might decrease cambial division and cell wall thickness (Piovesan et al., 2008), and prioritize carbon allocation to storage and mobilization of storage to support respiration rather than growth (Huang et al., 2021). On the other hand, this might not be a prioritization process but only the result of the direct impairment of cambial cell division by soil and atmospheric drought (Zweifel et al., 2021). In 2002, the increase in latewood percentage (WR; Fig. 3H) was more pronounced than for the other anatomical parameters, consistent with the previously reported high average climate sensitivity of this trait (Martin-Benito et al., 2013). During drought years, spruce trees indeed produce a denser wood (see CWRr in Fig. 3G; see also Soro et al., 2023a at the seedling stage) by forming latewood tracheids with smaller lumen and thicker walls (Huang et al., 2022; Soro et al., 2023b).

During the recovery phase, the production of tracheids with larger lumen diameters was coordinated with the decrease in water-use efficiency (Rc_LDr vs Rc_iWUE; Fig. 5). *Re*-growth of new xylem is the primary process by which trees recover their hydraulic conductivity after drought conditions (Brodribb et al., 2010; Arend et al., 2022), with the production of larger lumen conduits resulting in better hydraulic efficiency at a relatively low carbon cost (Tyree and Zimmermann, 2002). The significant and positive relationship between growth resilience (Rl_BAI) and iWUE resilience (Rl_iWUE) indicates that the most growth resilient families were also those able to most effectively change their water-use efficiency under drought conditions. In other words, families that best restore their growth after a drought are also those that maintain a higher iWUE during the post-stress period, and thus those

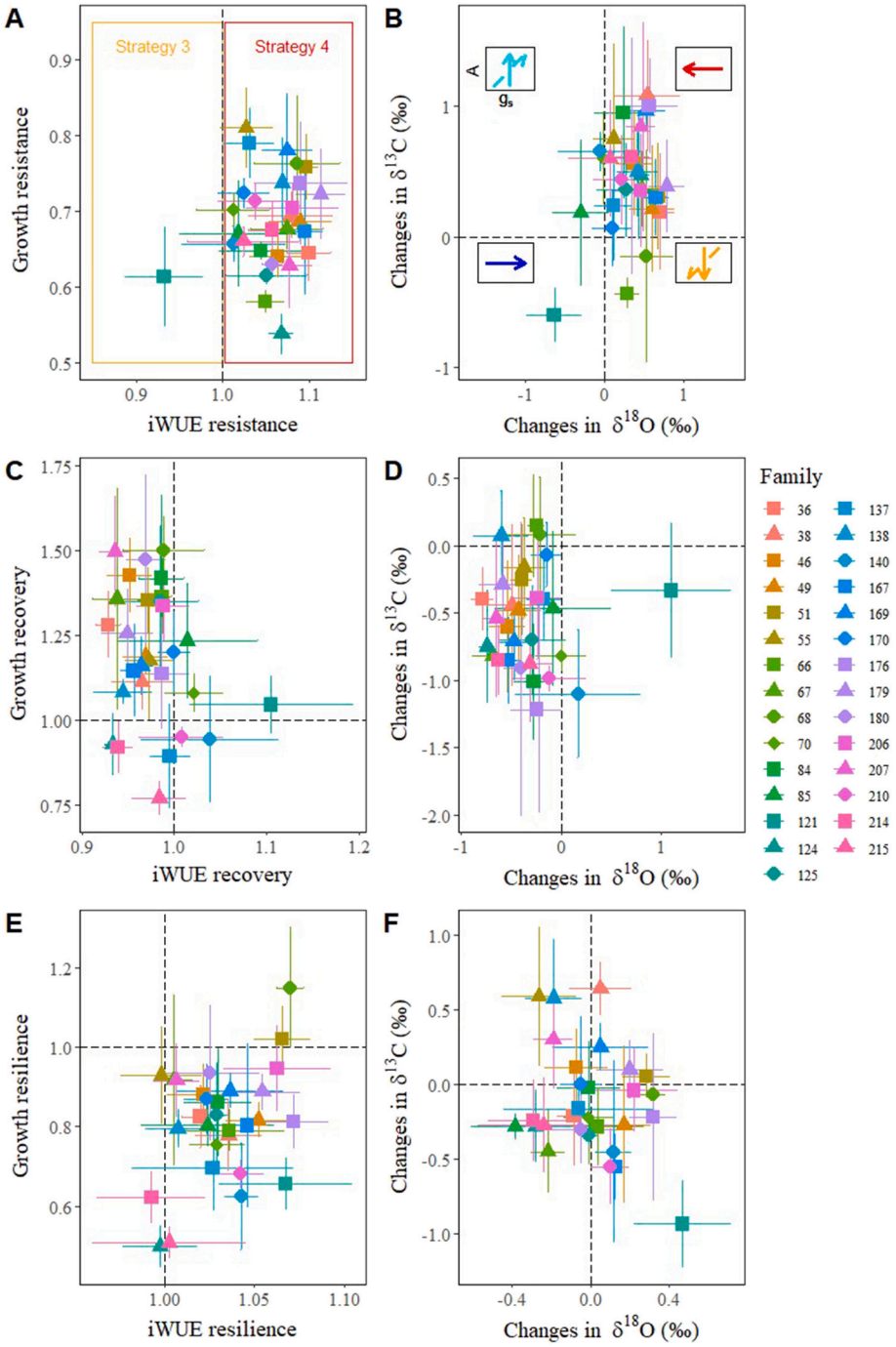

Fig. 4. Concomitant changes in growth and water-use efficiency, and carbon and oxygen isotope ratios of white spruce families in response to drought. The drought-response traits (i.e. resistance, recovery and resilience) derived from the basal area increment (BAI; abscissa axis) and the water-use efficiency (iWUE; ordinate axis) are presented in panels A, C and E. Concurrent changes in the carbon isotope results ($\delta^{13}C$) and oxygen isotope results ($\delta^{18}O$) in response to drought (i.e., pre-drought period versus drought, B), during the recovery phase (i.e., drought versus post-drought period, D) and for the difference between the pre-drought and the post-drought period (F) are presented in panels B, D and F. Data shown are mean values for white spruce families ± SE (N = 3–9). Families from the same natural geographical origin (called provenance or population) are presented with different symbols but with the same color. The insets in panel B present how the model proposed by Scheidegger et al. (2000) translates changes $\delta^{13}C$ and $\delta^{18}O$ changes to responses in stomatal conductance (gs) or photosynthetic capacity (A). The alternative interpretation for the orange and light blue scenarios is indicated by the dashed lines (Grams et al., 2007).

that least restore their pre-stress physiological capabilities. A high inter-annual plasticity in water-use efficiency is indicative of a more water-saving strategy, which can lead to a higher growth recovery or resilience, as shown in *Picea* and *Pinus* sp. (Forner et al., 2018; Wu et al., 2020).

4.2. *Isotopic results reveal different physiological strategies to cope with drought within populations*

The simultaneous analysis of $\delta^{18}O$ and $\delta^{13}C$ is crucial to understand the ecophysiological responses of trees, as it allows to discriminate whether changes observed in iWUE were attributed to variations of photosynthesis or stomatal conductance (Barbour, 2007). The rise in

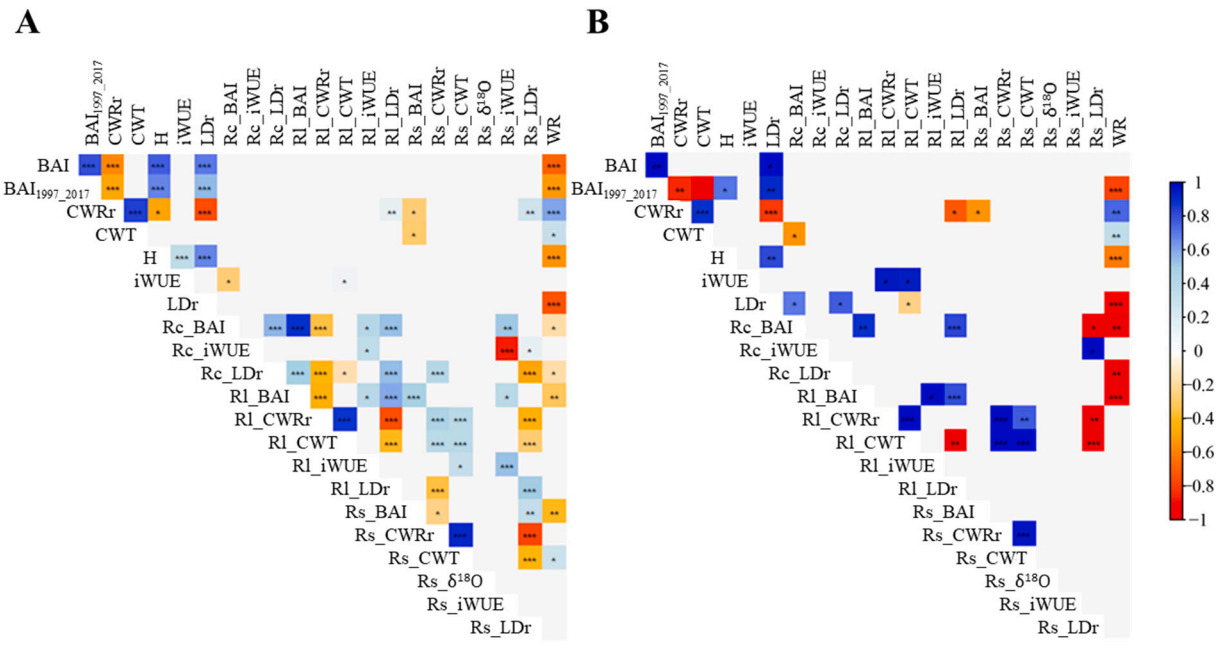

Fig. 5. Phenotypic and genetic correlations based on the most relevant traits analyzed in this study. (A) Pearson's phenotypic correlations were estimated based on family means of individual tree-ring trait values. The correlation coefficients are presented as defined in the color legend on the right side of the figure. (B) Estimated genetic correlations at the individual-tree level using the genomic-based GBLUP model for the white spruce families. In this figure, only the significant correlations are presented in color. The degrees of significance are represented by stars, as follows: *, $P < 0.05$; **, $P < 0.01$; ***, $P < 0.001$. For definitions of trait abbreviations, see Table 1.

Table 2
Variance components and narrow-sense heritability estimates for significantly heritable growth characteristics, wood anatomy, carbon isotopic composition, and drought-response traits. Variance components were obtained from for individual-tree linear mixed models ("GBLUP models", see Eq. [7]). When applicable, the type of data transformation is reported in the third column. The best model was chosen based on the Aikaike information criterion (AIC). $\overline{\sigma_p^2}$ and $\overline{\sigma_a^2}$ are the variance components associated with the plot and additive genetic effects, respectively, and averaged across years when applicable. Narrow-sense heritability (h^2) estimates and their standard errors (SE) are presented for each trait. Only traits with significant h^2 estimates are presented in this table.

Trait type	Trait name[a]	Data transformation	AIC	$\overline{\sigma_p^2}$	$\overline{\sigma_a^2}$	h^2 (SE)
Growth-related	BAI	square root	2106.605	2.822	24.044	0.449 (0.189)
Wood anatomy	CWT	log	2613.142	$3.601.10^{-4}$	$1.785.10^{-3}$	0.204 (0.039)
	LDr	log	−2942.282	$1.883.10^{-4}$	$5.723.10^{-3}$	0.789 (0.043)
	CWRr	log	1387.076	$3.537.\ 10^{-7}$	0.771	0.771 (0.029)
	WR	logit	504.458	0.00750	$7.131.10^{-2}$	0.391 (0.046)
Physiology-related	$\delta^{18}O$	–	369.027	$2.155.\ 10^{-3}$	0.1605	0.244 (0.051)
	$\delta^{13}C$	–	77.131	0.185	0.298	0.618 (0.043)
	iWUE	–	2704.689	21.550	34.752	0.617 (0.043)
Drought response	Rs_BAI	–	−405.118	$1.315.10^{-3}$	$6.774.10^{-3}$	0.650 (0.250)
	Rc_BAI	–	−135.803	$2.509.10^{-2}$	$5.518.10^{-2}$	0.627 (0.305)
	Rl_BAI	–	−212.8281	$8.913.10^{-3}$	$3.826.10^{-2}$	0.780 (0.271)
	Rl_CWT	–	−558.0699	$8.117.10^{-10}$	$2.433.10^{-3}$	0.827 (0.250)

[a] For definitions of trait abbreviations, see Table 1.

average intrinsic water-use efficiency (iWUE) seen across nearly all families during drought conditions (Fig. 4A), coupled with the increases in both $\delta^{18}O$ and $\delta^{13}C$ values (Fig. 3B), indicate that iWUE is primarily governed by stomatal conductance (Scheidegger et al., 2000). Our observations are in line with previous findings in white spruce (Saurer and Siegwolf, 2007). Under drought conditions, the significant stomatal closure observed in this conifer species, identified as an isohydric species (Sperry et al., 1994), restricts photosynthetic carbon assimilation, potentially resulting in an increase in maintenance respiration demands that may deplete carbohydrate reserves (McDowell et al., 2008). While stomatal conductance has a major role in regulating WUE in response to stress (Fig. 4B), the concurrent variations in $\delta^{13}C$ and $\delta^{18}O$ values during the post-drought period (Fig. 4D) indicate a physiological recovery strategy involving the regulation of stomatal conductance and assimilation rates.

Our dual-isotope analysis suggested that most white spruce families reacted to drought by small and non-significant variation of stomatal conductance and net carbon assimilation (Fig. 4B, D, F). In contrast with a previous study reporting a lack of intraspecific differences for iWUE response to drought in white spruce (Sinclair, 2019), here we report different physiological strategies between families within and among populations of the same tree species (Fig. 4). Of the eleven populations studied, five populations (POP_8, POP_11, POP_25, POP_34 and POP_42; Table S1) contained families with different physiological processes in response to stress (Fig. 4B; Table S5) and during the recovery phase (Fig. 4D; Table S5). Within a particularly low growth-resilient population (families 121, 124 and 125; POP_25), differences in processes were noted in response to drought, with trees in family 121 being unable to regulate their water use under stress conditions, while those in the family 124 substantially increased their iWUE (Fig. 4A-B; Table S5).

Similarly, two distinct families in a population originating from a relatively dry environment (families 51 and 55, POP_11) showed contrasting physiological strategies (Fig. 4B, F). The different physiological strategies inferred here among white spruce families suggest a diversity of water-use strategies within populations, as also observed for *Picea abies* (Hentschel et al., 2014). Indeed, conifer species appear to adopt multiple water- or carbon-use strategies in the face of drought, allowing them to be more highly resilient (Werner et al., 2021; Song et al., 2022). In evolutionary terms, rapid changes in environmental conditions could have exposed different cohorts within a population to different selection pressures, generating temporal differentiation in genetic constitution (Linhart and Grant, 1996). The diversity of physiological strategies observed among families, as well as the high tree-to-tree variation present within families (Fig. 4), are most likely linked to a high capacity for local adaptation to large climatic variations in white spruce. High genetic diversity for growth resilience to severe drought has already been observed among white spruce populations (Depardieu et al., 2020). Although these observations are consistent with *Picea glauca* being considered as one of the most adaptive conifer species in North America (Royer-Tardif et al., 2021), Lloret's index values for growth resilience were generally below 1 in our study, still suggesting a high vulnerability to future severe droughts, especially if drought episodes are becoming more prolonged or more frequent, beyond the minimum interval necessary for trees to recover from a single severe drought episode. In relation to this, little adaptive genetic variation was reported when white spruce trees from various seed sources faced a severe late spring frost after early-spring warming (Benomar et al., 2022), indicating the limits of genetic variation in such long-standing woody species in providing natural resistance to a succession of extreme climatic events, and the necessity to curb down global carbon emissions.

Though the Scheidegger/Grams approach provided insights into the physiological mechanisms involved in drought resistance and recovery, we acknowledge that specific assumptions had to be made (see Fig. 4). In this study, concurrent changes in $\delta^{18}O$ and $\delta^{13}C$ signatures were interpreted according to models developed from experimental data from three herbaceous species (Scheidegger et al., 2000), and leaf cellulose data from beech and spruce trees (Grams et al., 2007). Given that in our study, isotopic results were measured in tree rings, it is necessary to recall that stem growth can be fueled by carbohydrate reserves and/or fresh assimilates. Previous studies also demonstrated considerable time intervals between carbohydrate synthesis and utilization for cellulose production in the stem (Gessler et al., 2009, 2014; Offermann et al., 2011), implying that the isotopic values in tree rings are not necessarily synchronized with the timing of the water stress event, especially if the drought episode is intense or prolonged (Sarris et al., 2013). Previous observations suggested that using dual-isotope analysis and interpretations for carbon and oxygen isotope variations in tree rings might not entirely capture all potential shifts in the relationship between net assimilation and stomatal conductance (Roden and Farquhar, 2012; Roden et al., 2022). This indicates variability in the effectiveness of the dual-isotope approach across different environmental conditions and species (Roden and Farquhar, 2012). In this regard, the interpretation of our results might be taken with caution. Also, iWUE was measured at the whole-ring scale in our study, potentially masking significant iWUE responses at smaller scales despite earlywood representing around 70 % of the total ring in our dataset.

4.3. Conifer breeding for high water-use efficiency: prospects

To understand why some trees may be better adapted to future droughts than others, reliable adaptive traits linked to drought resilience need to be identified. In turn, trees or families could be selected for their higher drought tolerance in the context of breeding or reforestation purposes (Laverdière et al., 2022), which could be critical to preserve growth productivity as much as possible and also, enhance survival such as at the more vulnerable juvenile stage (Soro et al., 2023a). Carbon isotope ratios have been shown as a key indicator of drought stress in conifers due to the notable genetic variation among populations of the same species (Guy and Holowachuk, 2001; Warren et al., 2001), and the genetic control of functional traits related to iWUE drought response (de Miguel et al., 2014). iWUE was quite highly heritable in our study ($h^2 = 0.62$, Table 2). Other studies reported lower heritabilities for *Pinus pinaster* (0.23–0.41; Marguerit et al., 2023), *Pinus radiata* (0.07–0.20; Ismael et al., 2022) and *Picea mariana* (0.54; Johnsen et al., 1999). Although variability in heritability estimates depends on sites and experimental designs, and genetic variation in the sampled population, our heritability estimates are in line with those recently reported for *Picea glauca* (0.74–0.98; Cappa et al., 2022). In white spruce, $\delta^{13}C$ values were positively correlated to dry matter production or growth rates, thus highlighting the possibility to select genotypes for high iWUE without compromising yield (Sun et al., 1996; Cappa et al., 2022). Although iWUE was found to be heritable (Table 2), the lack of correlation between iWUE and long-term growth rates (Fig. 5A and B) does not support the idea that selecting more water-efficient trees would affect their performance in terms of wood production. Contrary to the idea that improving iWUE can not only be beneficial in drought-prone environments, but also promotes productivity under favorable conditions (Merchuck and Saranga, 2013), here we show that higher iWUE does not necessarily provide a growth advantage for white spruce trees. However, because of the genetic relationship between growth resilience and iWUE resilience, we suggest that spruce trees selected for higher resilience will bear the capacity to effectively adjust their water use under drought-stress conditions.

The major limitation of our study is that the traits analyzed may not be the key traits to explain the contrasting resilience indices observed among the 29 white spruce families analyzed herein. Studies exploring growth responses of conifer species using a broad range of functional traits are still scarce (but see Walters and Gerlach, 2013; Anderegg et al., 2018; Serra-Maluquer et al., 2022), and even fewer studies link the resultant trait spectra to differences in drought resilience across conifers (Gazol et al., 2017; Song et al., 2022), and even less at the intraspecific level. In response, the development of tools geared toward large-scale phenotypic screening related to drought response and recovery from severe climate events would be beneficial for advancing our knowledge on drought resilience. The use of state-of-the-art integrating approaches could couple isotope analysis (e.g., Moran et al., 2011) with other spatially and temporally intensive data collections obtained from whole genome or exome sequencing, genome-wide association studies, remote sensing, and high-throughput phenotyping platforms to decipher more precisely the physiological and genetic processes that determine drought resilience in trees.

5. Conclusions

In this study, we demonstrate that a precise assessment of the amplitude of response of wood traits to severe droughts provides a better understanding of the coordination of traits in response to stress and during the recovery phase, leading to a better understanding of the physiological mechanisms underlying drought resilience. For most white spruce families, the average increases in iWUE were likely driven by reductions in stomatal conductance. Our major finding is the presence of different groups reflecting various water-use strategies within white spruce populations. Considering that the timing, duration, and intensity of severe droughts have such a significant impact on a species' resistance and resilience (Aldea et al., 2022; Song et al., 2022), investigating the physiological response strategies of white spruce families in response to different severe droughts should be a focus of future studies. The presence of different groups reflecting different water-use strategies within tree species and within their local populations is likely to modulate the resilience of entire boreal forest ecosystems under future climate stress.

Supplementary data to this article can be found online at https://doi.

org/10.1016/j.scitotenv.2024.171174.

CRediT authorship contribution statement

Claire Depardieu: Conceptualization, Data curation, Formal analysis, Investigation, Methodology, Project administration, Resources, Software, Validation, Visualization, Writing – original draft, Writing – review & editing. **Patrick Lenz:** Conceptualization, Funding acquisition, Investigation, Project administration, Resources, Supervision, Validation, Writing – original draft, Writing – review & editing. **Joelle Marion:** Data curation, Formal analysis, Validation, Writing – review & editing. **Simon Nadeau:** Formal analysis, Investigation, Software, Validation, Visualization, Writing – original draft, Writing – review & editing. **Martin P. Girardin:** Formal analysis, Investigation, Validation, Visualization, Writing – original draft, Writing – review & editing. **William Marchand:** Data curation, Formal analysis, Investigation, Writing – review & editing. **Christian Bégin:** Investigation, Writing – review & editing. **Kerstin Treydte:** Writing – review & editing. **Arthur Gessler:** Conceptualization, Formal analysis, Validation, Writing – review & editing. **Jean Bousquet:** Conceptualization, Formal analysis, Funding acquisition, Investigation, Methodology, Project administration, Resources, Supervision, Validation, Writing – original draft, Writing – review & editing. **Martine M. Savard:** Investigation, Writing – review & editing. **Nathalie Isabel:** Conceptualization, Funding acquisition, Investigation, Methodology, Supervision, Validation, Writing – review & editing.

Declaration of competing interest

The authors have no conflicts of interest to declare that are relevant to the content of this article.

Data availability

The tree-ring data and R scripts are available on the Github website (https://github.com/ClaireDepardieu/Isotopes_drought_white_spruce). The original phenotypic data (basal area increment, wood anatomy, carbon and oxygen isotopes) are part of the network of the Natural Resources Canada white spruce genecological tests and common gardens, and have been stored in the Natural Resources Canada database (https://treesource.rncan.gc.ca). Full access can be shared upon request to the corresponding author or last author, according to the intellectual property policies of participating governmental institutions.

Acknowledgments

We thank Sébastien Gérardi (Univ. Laval), Lauriane Dinis (Natural Resources Canada), and Miriam Isaac-Renton (Natural Resources Canada) for constructive discussions. The authors are embedded to Marie-Claude Gros-Louis, Christine Simard, Philippe Labrie, Eric Dussault, Jean-François Légaré, and Vincent Seigner (Natural Resources Canada) for their assistance in the laboratory and field. We also thank Carole Coursolle (Natural Resources Canada) for language editing of the manuscript.

Funding

Support for this project was obtained from the Spruce-Up LSARP project (234FOR) funded by Genome Canada, Génome Québec and Genome British Columbia co-lead by J.B. and J. Bohlmann. Support was also provided by the Canada Research Chair in Forest Genomics and by a Natural Sciences and Engineering Research Council of Canada (NSERC) Discovery Grant to J.B., and GRDI funds from the Canadian Forest Service to N.I. and P.L.

References

Adams, H.D., Zeppel, M.J.B., Anderegg, W.R.L., et al., 2017. A multi-species synthesis of physiological mechanisms in drought-induced tree mortality. Nat. Ecol. Evol. 1, 1285–1291. https://doi.org/10.1038/s41559-017-0248-x.

Aldea, J., Ruiz-Peinado, R., del Rio, M., Pretzsch, H., Heym, M., Brazaitis, G., Jansons, A., Metslaid, M., Barbeito, I., Bielak, K., et al., 2022. Timing and duration of drought modulate tree growth response in pure and mixed stands of scots pine and Norway spruce. J. Ecol. 110 (11), 2673–2683. https://doi.org/10.1111/1365-2745.13978.

Anderegg, L.D., Berner, L.T., Badgley, G., Sethi, M.L., Law, B.E., HilleRisLambers, J., 2018. Within-species patterns challenge our understanding of the leaf economics spectrum. Ecol. Lett. 21, 734–744. https://doi.org/10.1111/ele.12945.

Arend, M., Link, R.M., Patthey, R., Kahmen, A., 2021. Rapid hydraulic collapse as cause of drought-induced mortality in conifers. Proc. Natl. Acad. Sci. USA 118 (16), e2025251118. https://doi.org/10.1073/pnas.2025251118.

Arend, M., Link, R.M., Zahnd, C., Hich, G., Schuldt, B., Kahmen, A., 2022. Lack of hydraulic recovery as a cause of post-drought foliage reduction and canopy decline in European beech. New Phytol. 234, 1195–1205. https://doi.org/10.1111/nph.18065.

Barbour, M.M., 2007. Stable oxygen isotope composition of plant tissue: a review. Funct. Plant Biol. 34, 83–94. https://doi.org/10.1071/fp06228.

Barbour, M.M., Andrews, T.J., Farquhar, G.D., 2001. Correlations between oxygen isotope ratios of wood constituents of *Quercus* and *Pinus* samples from around the world. Funct. Plant Biol. 28 (5), 335–348. https://doi.org/10.1071/PP00083.

Beaulieu, J., Nadeau, S., Ding, C., Celedon, J.M., Azaiez, A., Ritland, C., Laverdière, J.-P., Deslauriers, M., Adams, G., Fullarton, M., Bohlmann, J., Lenz, P., Bousquet, J., 2020. Genomic selection for resistance to spruce budworm in white spruce and relationships with growth and wood quality traits. Evol. Appl 13, 2704–2722. https://doi.org/10.1111/eva.13076.

Benomar, L., Lamhamedi, M.S., Rainville, A., Beaulieu, J., Bousquet, J., Margolis, H.A., 2016. Genetic adaptation vs. ecophysiological plasticity of photosynthetic-related traits in young *Picea glauca* trees along a regional climatic gradient. Front. Plant Sci. 7, 48 (15p.). https://doi.org/10.3389/fpls.2016.00048.

Benomar, L., Lamhamedi, M.S., Pépin, S., Rainville, A., Lambert, M.-C., Margolis, H.A., Bousquet, J., Beaulieu, J., 2018. Thermal acclimation of photosynbthesis and respiration of southern and northern white spruce seed sources along a regional climatic gradient indicates limited potential to cope with temperature warming. Ann. Bot. 121 (3), 443–457. https://doi.org/10.1093/aob/mcx174.

Benomar, L., Bousquet, J., Perron, M., Beaulieu, J., Lamara, M., 2022. Tree maladaptation under mid-latitude early spring warming and late cold spell: implications for assisted migration. Front. Plant Sci. 13 https://doi.org/10.3389/fpls.2022.920852, 920852 (12p.).

Brodribb, T.J., Cochard, H., 2009. Hydraulic failure defines the recovery and point of death in water-stressed conifers. Plant Physiol. 149, 575–584. https://doi.org/10.1104/pp.108.129783.

Brodribb, T.J., Bowman, D.J., Nichols, S., Delzon, S., Burlett, R., 2010. Xylem function and growth rate interact to determine recovery rates after exposure to extreme water deficit. New Phytol. 188, 533–542. https://doi.org/10.1111/j.1469-8137.2010.03393.

Brodribb, T.J., Powers, J., Cochard, H., Choat, B., 2020. Hanging by a thread? Forests and drought. Science 368 (6488), 261–266. https://doi.org/10.1126/science.aat7631.

Bunn, A.G., 2008. A dendrochronology program library in R (dplr). Dendrochronologia 26, 115–124. https://doi.org/10.1016/j.dendro.2008.01.002.

Butler, D.G., Cullis, B.R., Gilmour, A.R., Gogel, B.G., Thompson, R., 2017. ASReml-R Reference Manual Version 4, HP1. VSN International Ltd, Hemel Hempstead, UK, p. 1ES.

Camargo, A., 2022. PCAtest: testing the statistical significance of principal component analysis in R. PeerJ 10, e12967. https://doi.org/10.7717/peerj.12967.

Cappa, E.P., Klutsch, J.G., Sebastian-Azcona, J., Ratcliffe, B., Wei, X., Da Ros, L., Liu, Y., Chen, C., Benowicz, A., Sadoway, S., et al., 2022. Integrating genomic information and productivity and climate-adaptability traits into a regional white spruce breeding program. PLoS One 17 (3), e0264549. https://doi.org/10.1371/journal.pone.0264549.

Carminati, A., Javaux, M., 2020. Soil rather than xylem vulnerability controls stomatal response to drought. Trends Plant Sci. 25, 868–880. https://doi.org/10.1016/j.tplants.2020.04.0033.

Cheesman, A.W., Cernusak, L.A., 2017. Infidelity in the outback: climate signal recorded in $\Delta^{18}O$ of leaf but not branch cellulose of eucalypts across an Australian aridity gradient. Tree Physiol. 37, 554–564. https://doi.org/10.1093/treephys/tpw121.

Choat, B., Brodribb, T.J., Brodersen, C.R., Duursma, R.A., Lopez, R., Medlyn, B.E., 2018. Triggers of tree mortality under drought. Nature 558, 531–539. https://doi.org/10.1038/s41586-018-0240-x.

Core Team, 2022. R: A Language and Environment for Statistical Computing. R Foundation for Statistical Computing, Vienna, Austria. https://www.R-project.org/.

De La Torre, A.R., Sekhwal, M.K., Puiu, D., Salzberg, S.L., Scott, A.D., Allen, B., Neale, D. B., Chin, A.R.O., Buckley, T.N., 2022. Genome-wide association identifies candidate genes for drought tolerance in coast redwood and giant sequoia. Plant J. 109 (1), 7–22. https://doi.org/10.1111/tpj.15644.

de Miguel, M., Cabzas, J.-A., de María, N., Sánchez-Gómez, D., Guevara, M.-A., Vélez, M.-D., Sáez-Laguna, E., Díaz, L.-M., Mancha, J.-A., Barbero, M.-C., Collada, C., 2014. Genetic control of functional traits related to photosynthesis and water-use efficiency in *Pinus pinaster* Ait. Drought response: integration of genome annotation, allele association and QTL detection for candidate gene identification. BMC Genomics 15, 464. https://doi.org/10.1186/1471-2164-15-464.

Depardieu, C., Girardin, M.P., Nadeau, S., Lenz, P., Bousquet, J., Isabel, N., 2020. Adaptive genetic variation to drought in a widely distributed conifer suggests a potentiel for increasing forest resilience in a drying climate. New Phytol. 227 (2), 427–439. https://doi.org/10.1111/nph.16551.

Depardieu, C., Gérardi, S., Nadeau, S., Parent, G.J., Mackay, J., Lenz, P., Lamothe, M., Girardin, M.P., Bousquet, J., Isabel, N., 2021. Connecting tree-rings phenotypes, genetic associations and transcriptomics to decipher the genomic architecture of drought adaptation in a widespread conifer. Mol. Ecol. 30 (16), 3898–3917. https://doi.org/10.1111/mec.15846.

DeSoto, L., Cailleret, M., Sterck, F., Jansen, S., Kramer, K., et al., 2020. Low growth resilience to drought is related to future mortality risk in trees. Nat. Commun. 11, 545. https://doi.org/10.1038/s41467-020-14300-5.

Endelman, J.B., Jannink, J.L., 2012. Shrinkage estimation of the realized relationship matrix. G3-Genes Genom. Genet. 2, 1405–1413. https://doi.org/10.1534/g3.112.004259.

Farquhar, G.D., Richards, R.A., 1984. Isotopic composition of plant carbon correlates with water-use efficiency of wheat genotypes. Aust. J. Plant Physiol. 11, 539–552.

Farquhar, G.D., O'Leary, M.H., Berry, J.A., 1982. On the relationship between carbon isotope discrimination and the inter-cellular carbon-dioxide concentration in leaves. Aust. J. Plant Physiol. 9, 121–137.

Forner, A., Valladeres, F., Bonal, D., Granier, A., Grossiord, C., Aranda, I., 2018. Extreme droughts affecting Mediterranean tree species' growth and water-use efficiency: the importance of timing. Tree Physiol. 38 (8), 1127–1136. https://doi.org/10.1093/treephys/tpy022.

Gazol, A., Camarero, J., Anderegg, W., Vicente-Serrano, S., 2017. Impacts of droughts on the growth resilience of Northern Hemisphere forests. Glob. Ecol. Biogeogr. 26, 166–176. https://doi.org/10.1111/geb.12526.

George, J.-P., Grabner, M., Campelo, F., Karanitsch-Ackerl, S., Mayer, K., Klumpp, R.T., Schüler, S., 2019. Intra-specific variation in growth and wood density traits under water-limited conditions: long-term-, short-term-, and sudden responses of four conifer tree species. Sci. Total Environ. 660, 631–643. https://doi.org/10.1016/j.scitotenv.2018.12.478.

Gessler, A., Brandes, E., Buchmann, N., Helle, G., Rennenberg, H., Barnard, R.L., 2009. Tracing carbon and oxygen signals from newly assimilated sugars in the leaves to the tree-ring archive. Plant Cell Environ. 32, 780–795. https://doi.org/10.1111/j.1365-3040.2009.01957.x.

Gessler, A., Ferrio, J.P., Hommel, R., Treydte, K., Werner, R.A., Monson, R.K., 2014. Stable isotopes in tree rings: towards a mechanistic understanding of isotope fractionation and mixing processes from the leaves to the wood. Tree Physiol. 34 (8), 796–818. https://doi.org/10.1093/treephys/tpu040.

Gessler, A., Cailleret, M., Joseph, J., Schönbeck, L., Schaub, M., Lehmann, M., Rigling, A., Timofeeva, G., Saurer, M., 2018. Drought induced tree mortality: a tree-ring isotope based conceptual model to assess mechanisms and predispositions. New Phytol. 219, 485–490. https://doi.org/10.1111/nph.15154.

Gessler, A., Bottero, A., Marshall, J., Arend, M., 2020. The way back: recovery of trees from drought and its implication for acclimation. New Phytol. 228 (6), 1704–1709. https://doi.org/10.1111/nph.16703.

Grams, T.E.E., Kozovits, A.R., Häberle, K.-H., Matyssek, R., Dawson, T.E., 2007. Combining $\delta^{13}C$ and $\delta^{18}O$ analyses to unravel competition, CO_2 and O_3 effects on the physiological performance of different-aged trees. Plant Cell Environ. 30 (8), 1023–1034. https://doi.org/10.1111/j.1365-3040.2007.01696.x.

Graven, H., Allison, C.E., Etheridge, D.M., Hammer, S., Keeling, R.F., Levin, I., Meijer, H. A.J., 2017. Compiled records of carbon isotopes in atmospheric CO_2 for historical simulations in CMIP6. Geosci. Model Dev. 10, 4405–4417. https://doi.org/10.5194/gmd-10-4405-2017.

Guy, R.D., Holowachuk, D.L., 2001. Population differences in stable carbon isotope ratio of *Pinus contorta* Dougl. ex Loud.: relationship to environment, climate of origin, and growth potential. Can. J. Bot. 79 (3), 274–283. https://doi.org/10.1139/b01-001.

Hacke, U.G., Sperry, J.S., Pockman, W.P., Davis, S.D., McCulloh, K.A., 2001. Trends in wood density and structure are linked to prevention of xylem implosion by negative pressure. Oecologia 126, 457–461.

Hammond, W.M., Yu, K., Wilson, L.A., Will, R.E., Anderegg, W.R.L., Adams, H.D., 2019. Dead or dying? Quantifying the point of no return from hydraulic failure in drought-induced tree mortality. New Phytol. 223, 1834–1843. https://doi.org/10.1111/nph.15922.

Hassegawa, M., Savard, M., Lenz, P., Duchateau, E., Gélinas, N., Bousquet, J., Achim, A., 2020. White spruce wood quality for lumber products: priority traits and their enhancement through tree improvement. Forest. Int. J. Forest Res. 93 (1), 16–37. https://doi.org/10.1093/forestry/cpz050.

Hentschel, R., Rosner, S., Kayler, Z.E., Andreassen, K., Børja, I., Solberg, S., Tveito, O.E., Priesack, E., Gessler, A., 2014. Norway spruce physiological and anatomical predisposition to dieback. Forest Ecol. Manag. 322, 27–36. https://doi.org/10.1016/j.foreco.2014.03.007.

Hogg, E.H., Michaelian, M., Hook, T., Undershultz, M., 2017. Recent climatic drying leads to age-independent growth reductions of white spruce in stands in western Canada. Glob. Chang. Biol. 23 (12), 5297–5308. https://doi.org/10.1111/gcb.13795.

Holmes, R.L., 1983. Computer-assisted quality control in tree-ring dating and measuring. Tree-Ring Bull. 43, 69–78.

Housset, J.M., Nadeau, S., Isabel, N., Depardieu, C., Duchesne, I., Lenz, P., Girardin, M. P., 2018. Tree rings provide a new class of phenotypes that foster insights into adaptation of conifers to climate change. New Phytol. 218 (2), 630–645. https://doi.org/10.1111/nph.14968.

Huang, J., Hammerbacher, A., Gershenzon, J., Hartmann, H., 2021. Storage of carbon reserves in spruce trees is prioritized over growth in the face of carbon limitation. Proc. Natl. Acad. Sci. USA 118 (33), e2023297118. https://doi.org/10.1073/pnas.2023297118.

Huang, W., Fonti, P., Lundqvist, S.-O., Larsen, J., Hansen, J.K., Thygesen, L.G., 2022. Differences in xylem response to drought provide hints to future species selection. New For. 53, 759–777. https://doi.org/10.1007/s11056-021-09885-8.

Ibáñez, I., Acharya, K., Juno, E., Karounos, C., Lee, B.R., McCollum, C., et al., 2019. Forest resilience under global environmental change: do we have the information we need? A systematic review. PLoS ONE 14 (9), e0222207. https://doi.org/10.1371/journal.pone.0222207.

Ingrisch, J., Bahn, M., 2018. Towards a comparable quantification of resilience. Trends Ecol. Evol. 33, 251–259. https://doi.org/10.1016/j.tree.2018.01.013.

IPCC, 2021. Climate change 2021: the physical science basis. Contribution of working group I to the sixth assessment report of the intergovernmental panel on climate change [Masson-Delmotte, V., P. Zhai, A. Pirani, S.L. Connors, C. Péan, S. Berger, N. Caud, Y. Chen, L. Goldfarb, M.I. Gomis, M. Huang, K. Leitzell, E. Lonnoy, J.B.R. Matthews, T.K. Maycock, T. Waterfield, O. Yelekçi, R. Yu, and B. Zhou (eds.)]. Cambridge University Press.

Isaac-Renton, M., Montwé, D., Hamann, A., Spiecker, H., Cherubini, P., Treydte, K., 2018. Northern forest tree populations are physiologically maladapted to drought. Nat. Commun. 9, 5254. https://doi.org/10.1038/s41467-018-07701-0.

Ismael, A., Xue, J., Meason, D.F., Klápště, J., Gallart, M., Li, Y., Bellè, P., Gomez-Gallego, M., Bradford, K.T., Telfer, E., Dungey, H., 2022. Genetic variation in drought-tolerance traits and their relationships to growth in *Pinus radiata* D. Don under water stress. Front. Plant Sci. https://doi.org/10.3389/fpls.2021.766803.

Johnsen, K.H., Flanagan, L., Huber, D.A., Major, J.E., 1999. Genetic variation in growth, carbon isotope discrimination, and foliar N concentration in *Picea mariana*: analyses from a half-diallel mating design using field-grown trees. Can. J. For. Res. 29 (11), 1727–1735. https://doi.org/10.1139/cjfr-29-11-1727.

Keeling, R.F., Piper, S.C., Bollenbacher, A.F., Walker, J.S., 2009. Atmospheric CO_2 Records from Sites in the SIO Air Sampling Network. In Trends: A Compendium of Data on Global Change. Carbon Dioxide Information Analysis Center, oak Ridge National Laboratory, U.S. Department of Energy, Oak Ridge, Tenn., U.S.A. https://doi.org/10.3334/CDIAC/atg.035.

Klesse, S., Babst, F., Evans, M.E.K., Hurley, A., Pappas, C., Peters, R.L., 2023. Legacy effects in radial tree growth are rarely significant after accounting for biological memory. J. Ecol. 111, 1188–1202. https://doi.org/10.1111/1365-2745.14045.

Kruse, J., Hopmans, P., Renneberg, H., Adams, M., 2012. Modern tools to tackle traditional concerns: evaluation of site productivity and *Pinus radiata* management via $\delta^{13}C$ and $\delta^{18}O$ analysis in tree-rings. For. Ecol. Manag. 285, 227–238. https://doi.org/10.1016/j.foreco.2012.08.011.

Lapenis, A., Robinson, G.R., Lawrence, G.B., 2022. Radial growth decline of white spruce (*Picea glauca*) during hot summers without drought: preliminary results from a study site south of a boreal forest border. Can. J. For. Res. 52 (4) https://doi.org/10.1139/cjfr-2021-0268.

Laverdière, J.P., Lenz, P., Nadeau, S., Depardieu, C., Isabel, N., Perron, M., Beaulieu, J., Bousquet, J., 2022. Breeding for adaptation to climate change: genomic selection for drought response in a white spruce multi-site polycross test. Evol. Appl. 15 (3), 383–402. https://doi.org/10.1111/eva.13348.

Li, P., Beaulieu, J., Corriveau, A., Bousquet, J., 1993. Genetic variation in juvenile growth and phenology in a white spruce provenance-progeny test. Silvae Genet. 42 (1), 52–60.

Li, P., Beaulieu, J., Bousquet, J., 1997. Genetic structure and patterns of genetic variation among populations in eastern white spruce (*Picea glauca*). Can. J. For. Res. 27, 189–198.

Linhart, Y.B., Grant, M.C., 1996. Evolutionary significance of local genetic differentiation in plants. Annu. Rev. Ecol. Evol. Syst. 27, 237–277.

Lloret, F., Keeling, E.G., Sala, A., 2011. Components of tree resilience: effects of successive low-growth episodes in old ponderosa pine forests. Oikos 120 (2), 1909–1920. https://doi.org/10.1111/j.1600-0706.2011.19372.x.

Marguerit, E., Bouffier, L., Chancerel, E., Costa, P., Lagane, F., Guehl, J.-M., Plomion, C., Brendel, O., 2023. The genetics of water-use efficiency and its relation to growth in maritime pine. J. Exp. Bot. 65, 4757–4768. https://doi.org/10.1093/jxb/eru226.

Martin-Benito, D., Beeckman, H., Cañellas, I., 2013. Influence of drought on tree rings and tracheid features of *Pinus nigra* and *Pinus sylvestris* in a Mesic Mediterranean forest. Eur. J. For. Res. 132, 33–45. https://doi.org/10.1007/s10342-012-0652-3.

Martinez-Meier, A., Sanchez, L., Pastorino, M., Gallo, L., Rozenberg, P., 2008. What is hot in tree rings? The wood density of surviving Douglas-firs to the 2003 drought and heat wave. For. Ecol. Manag. 256 (4), 837–843. https://doi.org/10.1016/j.foreco.2008.05.041.

McDowell, N., Pockman, W.T., Allen, C.D., Bresheras, D.D., Cobb, N., Kolb, T., Plaut, J., Sperry, J., West, A., Williams, D.G., Yepez, E.A., 2008. Mechanisms of plant survival and mortality during drought: why do some plants survive while others succumb to drought? New Phytol. 178 (4), 719–739. https://doi.org/10.1111/j.1469-8137.2008.02436.x.

McDowell, N.G., Sevanto, S., 2010. The mechanisms of carbon starvation: how, when, or does it even occur at all? New Phytol. 186 (2), 264–266. https://doi.org/10.1111/j.1469-8137.2010.03232.x.

Merchuck, L., Saranga, Y., 2013. Breeding approaches to increasing water-use efficiency. In: Regel, Z. (Eds.), Improving Water and Nutrient-Use Efficiency in Food Production Systems. John Wiley & Sons, Inc., pp. 145–160. doi:https://doi.org/10.1002/9781118517994.ch9.

Mirabel, A., Girardin, M.P., Metsaranta, J., Way, D., Reich, P.B., 2023. Increasing atmospheric dryness reduces boreal forest tree growth. Nat. Commun. 14, 6901. https://doi.org/10.1038/s41467-023-42466-1.

Moran, J.J., Newburn, M.K., Alexander, M.L., Sams, R.L., Kelly, J.E., Kreuzer, H.W., 2011. Laser ablation isotope ratio mas spectrometry for enhanced sensitivity and

spatial resolution in stable isotope analysis. Rapid Commun. Mass Spectrom. 25 (9), 1282–1290. https://doi.org/10.1002/rcm.4985.
Munson, S.M., Bradford, J.B., Hultine, K.R., 2021. An integrative ecological drought framework to span plant stress to ecosystem transformation. Ecosystems 24, 739–754. https://doi.org/10.1007/s10021-020-00555-y.
Nikinmaa, L., Lindner, M., Cantarello, E., Jump, A.S., Seidl, R., Winkel, G., Muys, B., 2020. Reviewing the use of resilience concepts in forest sciences. Curr. Forest. Rep. 6, 61–80. https://doi.org/10.1007/s40725-020-00110-x.
Nolan, R.H., Gauthey, A., Losso, A., Medlyn, B.E., Smith, R., Chhajed, S.S., Fuller, K., Song, M., Li, X., Beaumont, L.J., et al., 2021. Hydraulic failure and tree size linked with canopy die-back in eucalypt forest during extreme drought. New Phytol. 230 (4), 1354–1365. https://doi.org/10.1111/nph.17298.
Offermann, C., Ferrio, J.P., Holst, J., Grote, R., Siegwolf, R., Kayler, Z., Gessler, A., 2011. The long way down—are carbon and oxygen isotope signals in the tree ring uncoupled from canopy physiological processes? Tree Physiol. 31, 1088–1102. https://doi.org/10.1093/treephys/tpr093.
Pellizari, E., Camarero, J.J., Gazol, A., Sanguesa-Barreda, G., Carrer, M., 2016. Wood anatomy and carbon-isotope discrimination support long-term hydraulic deterioration as a major cause of drought-induced dieback. Glob. Chang. Biol. 22 (6), 2125–2137. https://doi.org/10.1111/gcb.13227.
Peng, C., Ma, Z., Lei, X., Zhu, Q., Chen, H., Wang, W., et al., 2011. A drought-induced pervasive increase in tree mortality across Canada's boreal forests. Nat. Clim. Chang. 1 (9), 467–471. https://doi.org/10.1038/Nclimate1293.
Piovesan, G., Biondi, F., Di Filippo, A., Alessandrini, A., Maugeri, M., 2008. Drought-driven growth reduction in old beech (*Fagus sylvatica*) forests of the central Apennines, Italy. Glob. Chang. Biol. 14, 1265–1281. https://doi.org/10.1111/j.1365-2486.2008.01570.x.
Pittermann, J., Sperry, J.S., Wheeler, J.K., Hacke, U.G., Sikkema, E.H., 2006. Mechanical reinforcement of tracheids compromises the hydraulic efficiency of conifer xylem. Plant Cell Environ. 29, 1618–1628. https://doi.org/10.1111/j.1365-3040.2006.01539.x.
Puchi, P.F., Camarero, J.J., Carrer, M., 2021. Retrospective analysis of wood anatomical traits and tree-ring isotopes suggests site-specific mechanisms triggering *Araucaria araucana* drought-induced dieback. Glo. Chang. Biol. 27, 6394–6408. https://doi.org/10.1111/gcb.15881.
Reich, P.B., Sendall, K.M., Stefanski, A., Rich, R.L., Hobbie, S.E., Montgomery, R.A., 2018. Effects of climate warming on photosynthesis in boreal tree species depend on soil moisture. Nature 562, 263–267. https://doi.org/10.1038/s41586-018-0582-4.
Roden, J., Saurer, M., Siegwolf, R.T., 2022. Probing tree physiology using the dual-isotope approach. In: Stable Isotopes in Tree Rings: Inferring Physiological, Climatic and Environmental Responses. Springer International Publishing, Cham, pp. 463–479.
Roden, J.S., Farquhar, G.D., 2012. A controlled test of the dual-isotope approach for the interpretation of stable carbon and oxygen isotope ratio variation in tree rings. Tree Physiol. 32 (4), 490–503. https://doi.org/10.1093/treephys/tps019.
Royer-Tardif, S., Boisvert-Marsh, L., Godbout, J., Isabel, N., Aubin, I., 2021. Finding common ground: toward comparable indicators of adaptive capacity of tree species to a changing climate. Ecol. Evol. 11, 13081–13100. https://doi.org/10.1002/ece3.8024.
Ruehr, N.K., Grote, R., Mayr, S., Arneth, A., 2019. Beyond the extreme: recovery of carbon and water relations in woody plants following heat and drought stress. Tree Physiol. 39, 1285–1299. https://doi.org/10.1093/treephys/tpz032.
Sang, Z., Sebastian-Azcona, J., Hamann, A., Menzel, A., Hacke, U., 2019. Adaptive limitations of white spruce populations to drought imply vulnerability to climate change in its western range. Evol. Appl. 12 (9), 1850–1860. https://doi.org/10.1111/eva.12845.
Sarris, D., Siegwolf, R., Körner, C., 2013. Inter- and intra-annual stable carbon and oxygen isotope signals in response to drought in two Mediterranean pines. Agric. For. Meteorol. 168, 59–68. https://doi.org/10.1016/j.agrformet.2012.08.007.
Saurer, M., Siegwolf, R.T.W., 2007. Human impacts on tree-ring growth reconstructed from stable isotopes, terrestrial ecology, Elsevier, 1, 49-62, ISSN 1936-7961. ISBN 9780123736277. https://doi.org/10.1016/S1936-7961(07)01004-4.
Scheidegger, Y., Saurer, M., Bahn, M., Siegwolf, R.T.W., 2000. Linking stable oxygen and carbon isotopes with stomatal conductance and photosynthetic capacity: a conceptual model. Oecologia 125, 350–357. https://doi.org/10.1007/s004420000466.
Schueler, S., George, J.-P., Karanitsch-Ackerl, S., Mayer, K., Klumpp, R.T., Grabner, M., 2021. Evolvability of drought response in four native and non-native conifers: opportunities for forest and genetic resource management in Europe. Front. Plant Sci. 12 https://doi.org/10.3389/fpls.2021.648312.
Serra-Maluquer, X., Gazol, A., Anderegg, W.R.L., Martínez-Vilalta, J., Mencuccini, M., Camarero, J.J., 2022. Wood density and hydraulic traits influence species' growth response to drought across biomes. Glob. Chang. Biol. 28, 3871–3882. https://doi.org/10.1111/gcb.16123.
Sevanto, S., McDowell, N.G., Dickman, L.T., Pangle, R., Pockman, W.T., 2014. How do trees die? A test of the hydraulic failure and carbon starvation hypotheses. Plant Cell Environ. 37, 153–161. https://doi.org/10.1111/pce.12141.
Sinclair, L., 2019. A range-wide common garden experiment of white spruce indicates population differentiation in drought tolerance traits. ERA. Available at. https://doi.org/10.7939/r3-tpca-bn95.
Song, Y., Sterck, F., Zhou, X., Liu, Q., Kruijt, B., Poorter, L., 2022. Drought resilience of conifer species is driven by leaf lifespan but not hydraulic traits. New Phytol. 235 (3), 978–992. https://doi.org/10.1111/nph.18177.
Soro, A., Lenz, P., Roussel, J.-R., Larochelle, F., Bousquet, J., Achim, A., 2023a. The phenotypic ad genetic effects of drought-induced stress on apical growth, ring width, wood density and biomass of white spruce seedlings. New For. 54, 789–811. https://doi.org/10.1007/s11056-022-09939-5.
Soro, A., Lenz, P., Roussel, J.-R., Nadeau, S., Pothier, D., Bousquet, J., Achim, A., 2023b. The phenotypic ad genetic effects of drought-induced stress on wood specific conductivity and anatomical properties in white spruce seedlings and relationships with growth and wood density. Front. Plant Sci. 14, 1297314 (17p.). doi:https://doi.org/10.3389/fpls.2023.1297314.
Sperry, J.S., Nichols, K.L., Sullivan, J.E.M., Eastlack, S., 1994. Xylem embolism in ring-porous, diffuse-porous, and coniferous trees of northern Utah and interior Alaska. Ecology 75, 1736–1752.
Sun, Z.J., Livingston, N.J., Guy, R.D., Ethier, G.J., 1996. Stable carbon isotopes as indicators of increased water-use efficiency and productivity in white spruce (*Picea glauca* (Moench) Voss) seedlings. Plant Cell Environ. 19 (7), 887–894. https://doi.org/10.1111/j.1365-3040.1996.tb00425.x.
Tyree, M.T., Zimmermann, M.H., 2002. Xylem Structure and the Ascent of Sap, 2nd edition. Springer, Berlin, Germany. https://link.springer.com/book/10.1007/978-3-662-04931-0.
Vicente-Serrano, S.M., Quiring, S.M., Peña-Gallardo, M., Yuan, S., Domínguez-Castro, F., 2020. A review of environmental droughts: increased risk under global warming? Earth Sci. Rev. 201, 102953 https://doi.org/10.1016/j.earscirev.2019.102953.
Voelker, S.L., Merschel, A.G., Meinzer, F.C., Ulrich, D.E.M., Spies, T.A., Still, C.J., 2019. Fire deficits have increased drought sensitivity in dry conifer forests: fire frequency and tree-ring carbon isotope evidence from Central Oregon. Glob. Chang. Biol. 25, 1247–1262. https://doi.org/10.1111/gcb.14543.
Voltas, J., Camarero, J.J., Carulla, D., Aguilera, M., Ortiz, A., Ferrio, J.P., 2013. A retrospective, dual-isotope approach reveals individual predispositions to winter-drought induced tree dieback in the southernmost distribution limit of scots pine. Plant Cell Environ. 36 (8), 1435–1448. https://doi.org/10.1111/pce.12072.
Walters, M.B., Gerlach, J.P., 2013. Intraspecific growth and functional leaf trait responses to natural soil resource gradients for conifer species with contrasting leaf habit. Tree Physiol. 33, 297–310. https://doi.org/10.1093/treephys/tps134.
Wang, W., English, N.B., Grossiord, C., Gessler, A., Das, A.J., Stephenson, N.L., Baisan, C. H., Allen, C.D.M. McDowell, N.G., 2021. Mortality predispositions of conifers across western USA. New Phytol. 229 (2), 831–844. https://doi.org/10.1111/nph.16864.
Warren, C.R., McGrath, J.F., Adams, M.A., 2001. Water availability and carbon isotope discrimination in conifers. Oecologia 127, 476–486. https://doi.org/10.1007/s004420000609.
Wei, T., Simko, V., 2017. R package "corrplot": Visualization of a Correlation Matrix (Version 0.84). Available from. https://github.com/taiyun/corrplot.
Weigt, R.B., Braulich, S., Zimmermann, L., Saurer, M., Grams, T.E.E., Dietrich, H.D., Siegwolf, R.T.W., Nikolova, P.S., 2015. Comparaison of $\delta^{18}O$ and $\delta^{13}C$ values between tree-ring whole wood and cellulose in five species growing under two different site conditions. Rapid Commun. Mass Spectrom. 29, 2233–2244. https://doi.org/10.1002/rcm.7388.
Werner, C., Meredith, L.K., Ladd, S.N., Ingrisch, J., Kübert, A., Haren, J.V., Bahn, M., Bailey, K., Bamberger, I., et al., 2021. Ecosystem fluxes during drought and recovery in an experimental forest. Science 374, 6574. https://doi.org/10.1126/science.abj6789.
Wheaton, E., Kulshreshtha, S., Wittrock, V., Koshida, G., 2008. Dry times: hard lessons from the Canadian drought of 2001 and 2002. Can. Geogr. 52, 241–262. https://doi.org/10.1111/j.1541-0064.2008.00211.x.
Wu, G., Liu, X., Chen, T., Xu, G., Wang, B., Kang, H., Li, C., Zeng, X., 2020. The positive contribution of iWUE to the resilience of Schrenk spruce (*Picea schrenkiana*) to extreme drought in the western Tianshan Mountains. China. Acta Physiol. Plant. 42, 168. https://doi.org/10.1007/s11738-020-03158-1.
Zas, R., Sampedro, L., Solla, A., Vivas, M., Lombardero, M.J., Alia, R., Rozas, V., 2020. Dendroecology in common gardens: population differentiation and plasticity in resistance, recovery and resilience to extreme drought events in *Pinus pinaster*. Agric. For. Meteorol. 291, 108060 https://doi.org/10.1016/j.agrformet.2020.108060.
Zhang, J.W., Cregg, B.M., 1996. Variation in stable carbon isotope discrimination among and within exotic conifer species grown in eastern Nebraska. USA. For. Ecol. Manag. 83 (3), 181–187. https://doi.org/10.1016/0378-1127(96)03723-1.
Zweifel, R., Sterck, F., Braun, S., Buchmann, N., Eugster, W., Gessler, A., Häni, M., Peters, R.L., Walthert, L., Wilhelm, M., et al., 2021. Why trees grow at night. New Phytol. 231 (6), 2174–2185. https://doi.org/10.1111/nph.17552.